

Odd entanglement entropy in $\overline{\text{T}\overline{\text{T}}}$ deformed CFT_2 s and holography

Debarshi Basu^{ⓧ,*}, Saikat Biswas^{ⓧ,†}, Ankur Dey,[‡] Boudhayan Paul^{ⓧ,§} and Gautam Sengupta^{||}
Department of Physics, Indian Institute of Technology, Kanpur 208 016, India

 (Received 9 August 2023; accepted 24 November 2023; published 15 December 2023)

We construct a replica technique to perturbatively compute the odd entanglement entropy (OEE) for bipartite mixed states in $\overline{\text{T}\overline{\text{T}}}$ deformed CFT_2 s. This framework is then utilized to obtain the leading-order correction to the OEE for two disjoint intervals, two adjacent intervals, and a single interval in $\overline{\text{T}\overline{\text{T}}}$ deformed thermal CFT_2 s in the large central charge limit. The field theory results are subsequently reproduced in the high-temperature limit from holographic computations for the entanglement wedge cross sections in the dual bulk finite cutoff Bañados-Teitelboim-Zanelli geometries. We further show that for finite size $\overline{\text{T}\overline{\text{T}}}$ deformed CFT_2 s at zero temperature the corrections to the OEE are vanishing to the leading order from both field theory and bulk holographic computations.

DOI: 10.1103/PhysRevD.108.126013

I. INTRODUCTION

Quantum entanglement has emerged as a prominent area of research to explore a wide range of physical phenomena spanning several disciplines from quantum many-body systems in condensed matter physics to issues of quantum gravity and black holes. The entanglement entropy (EE) has played a crucial role in this endeavor as a measure for characterizing the entanglement of bipartite pure quantum states although it fails to effectively capture mixed-state entanglement due to spurious correlations. In this context several mixed-state entanglement and correlation measures such as the reflected entropy, entanglement of purification, balanced partial entanglement etc. have been proposed in quantum information theory.

Interestingly it was possible to compute several of these measures through certain replica techniques for bipartite states in two-dimensional conformal field theories (CFT_2 s). In this connection the Ryu-Takayanagi (RT) proposal [1,2] quantitatively characterized the holographic entanglement entropy (HEE) of a subsystem in CFT s dual to bulk AdS geometries through the AdS/CFT correspondence. This was extended by the Hubeny-Rangamani-Takayanagi (HRT) proposal [3] which provided a covariant generalization of

the RT proposal for time dependent states in CFT s dual to nonstatic bulk AdS geometries. The RT and HRT proposals were later proved in [4–7].

Recently another computable measure for mixed state entanglement known as the odd entanglement entropy (OEE) was proposed by Tamaoka in [8]. The OEE may be broadly understood as the von Neumann entropy of the partially transposed reduced density matrix of a given subsystem [8].¹ The author in [8] utilized a suitable replica technique to compute the OEE for a bipartite mixed state configuration of two disjoint intervals in a CFT_2 . Interestingly in [8] the author proposed a holographic duality relating the OEE and the EE to the bulk-entanglement wedge cross section (EWCS) for a given bipartite state in the $\text{AdS}_3/\text{CFT}_2$ scenario. For recent developments see [9–18].

On a different note it was demonstrated by Zamolodchikov [19] that CFT_2 s which have undergone an irrelevant deformation by the determinant of the stress tensor (known as $\overline{\text{T}\overline{\text{T}}}$ deformations) exhibit exactly solvable energy spectrum and partition function. These theories display nonlocal UV structure and have an infinite number of possible RG flows leading to the same fixed point. A holographic dual for such theories was proposed in [20] to be a bulk AdS_3 geometry with a finite radial cutoff. This proposal could be substantiated through the matching of the two-point function, energy spectrum and the partition function between the bulk and the boundary (see [21–29] for further developments). The authors in [30–40] computed the HEE for bipartite pure state

*debarshi@iitk.ac.in

†saikatb21@iitk.ac.in

‡ankurd21@iitk.ac.in

§paul@iitk.ac.in

||sengupta@iitk.ac.in

Published by the American Physical Society under the terms of the *Creative Commons Attribution 4.0 International* license. Further distribution of this work must maintain attribution to the author(s) and the published article's title, journal citation, and DOI. Funded by SCOAP³.

¹This is a loose interpretation as the partially transposed reduced density matrix does not represent a physical state and may contain negative eigenvalues [8].

configurations in various $T\bar{T}$ deformed dual CFTs. Subsequently the authors in [41] obtained the reflected entropy and its holographic dual, the EWCS, for bipartite mixed states in $T\bar{T}$ deformed dual CFT₂s. Recently the entanglement negativity for various bipartite mixed states in $T\bar{T}$ deformed thermal CFT₂s, and the corresponding holographic dual for bulk finite cutoff Bañados-Teitelboim-Zanelli (BTZ) black hole geometries were computed in [42].

Motivated by the developments described above, in this article we compute the OEE for various bipartite mixed states in $T\bar{T}$ deformed dual CFT₂s. For this purpose we construct an appropriate replica technique and a conformal perturbation theory along the lines of [32,34,42] to develop a path integral formulation for the OEE in $T\bar{T}$ deformed CFT₂s with a small deformation parameter. This perturbative construction is then utilized to compute the first-order corrections to the OEE for two disjoint intervals, two adjacent intervals, and a single interval in a $T\bar{T}$ deformed thermal CFT₂ with a small deformation parameter in the large central charge limit. Subsequently we explicitly compute the bulk EWCS for the above mixed-state configurations in the $T\bar{T}$ deformed thermal dual CFT₂s by employing a construction involving embedding coordinates as described in [10]. Utilizing the EWCS obtained we demonstrate that the first-order correction to field theory replica technique results for the OEE in the large central charge and the high-temperature limit match exactly with the first-order correction to the sum of the EWCS and the HEE verifying the holographic duality between the above quantities in the context of $T\bar{T}$ deformed thermal CFT₂s. Following this we extend our perturbative construction to $T\bar{T}$ deformed finite size CFT₂s at zero temperature and demonstrate that the leading-order corrections to the OEE are vanishing, which is substantiated through bulk holographic computations involving the EWCS.

This article is organized as follows. In Sec. II we briefly review the basic features of $T\bar{T}$ deformed CFT₂s and the OEE. In Sec. III we develop a perturbative expansion for the OEE in a $T\bar{T}$ deformed CFT₂. In Sec. IV this perturbative construction is then employed to obtain the leading-order corrections to the OEE for various bipartite states in a $T\bar{T}$ deformed thermal CFT₂. Following this we explicitly demonstrate the holographic duality for first-order corrections between the OEE and the sum of the bulk EWCS and the HEE for these mixed states. Subsequently in Sec. V we extend our perturbative analysis to a $T\bar{T}$ deformed finite size CFT₂ at zero temperature and show that the leading-order corrections to the OEE are zero. This is later verified through bulk holographic computations. Finally, we summarize our results in Sec. VI and present our conclusions. Some of the lengthy technical details of our computations have been described in Appendix.

II. REVIEW OF EARLIER LITERATURE

A. $T\bar{T}$ deformation in a CFT₂

We begin with a brief review of a two-dimensional conformal field theory deformed by the $T\bar{T}$ operator defined as follows [19]:

$$(T\bar{T}) = \frac{1}{8}(T_{ab}T^{ab} - (T_a^a)^2). \quad (2.1)$$

It is a double-trace composite operator which satisfies the factorization property [19]. The corresponding deformation generates a one parameter family of theories described by a deformation parameter $\mu(\geq 0)$ as given by the following flow equation [19,32,34]:

$$\frac{d\mathcal{I}_{\text{QFT}}^{(\mu)}}{d\mu} = \int d^2x (T\bar{T})_{\mu}, \quad \mathcal{I}_{\text{QFT}}^{(\mu)}|_{\mu=0} = \mathcal{I}_{\text{CFT}}, \quad (2.2)$$

where $\mathcal{I}_{\text{QFT}}^{(\mu)}$ and \mathcal{I}_{CFT} represent the actions of the deformed and undeformed theories respectively. The deformation parameter μ has dimensions of length squared. Note that the energy spectrum may be determined exactly for a $T\bar{T}$ deformed CFT₂ [43,44].

When μ is small, the action of the deformed CFT₂ may be perturbatively expanded as [32,34]

$$\begin{aligned} \mathcal{I}_{\text{QFT}}^{(\mu)} &= \mathcal{I}_{\text{CFT}} + \mu \int d^2x (T\bar{T})_{\mu=0} \\ &= \mathcal{I}_{\text{CFT}} + \mu \int d^2x (T\bar{T} - \Theta^2), \end{aligned} \quad (2.3)$$

where $T \equiv T_{ww}$, $\bar{T} \equiv T_{\bar{w}\bar{w}}$, and $\Theta \equiv T_{w\bar{w}}$ describe the components of the stress tensor of the undeformed theory expressed in the complex coordinates (w, \bar{w}) . Our investigation focuses on deformed CFT₂s at a finite-temperature, and finite-size deformed CFT₂s at zero temperature, which are defined on appropriate cylinders. The expectation value of Θ vanishes on a cylinder and the Θ^2 term in Eq. (2.3) may be dropped from further consideration [32].

B. Odd entanglement entropy

We now focus our attention on a bipartite mixed state correlation measure termed the OEE, which approximately characterizes the von Neumann entropy for the partially transposed reduced density matrix of a given bipartite system [8]. In this context we begin with a bipartite system comprising the subsystems A and B , described by the reduced density matrix ρ_{AB} defined on the Hilbert space $\mathcal{H}_{AB} = \mathcal{H}_A \otimes \mathcal{H}_B$, where \mathcal{H}_A and \mathcal{H}_B denote the Hilbert spaces for the subsystems A and B , respectively. The partial transpose $\rho_{AB}^{T_B}$ for the reduced density matrix ρ_{AB} with respect to the subsystem B is then given by

$$\langle e_i^{(A)} e_j^{(B)} | \rho_{AB}^{T_B} | e_k^{(A)} e_l^{(B)} \rangle = \langle e_i^{(A)} e_l^{(B)} | \rho_{AB} | e_k^{(A)} e_j^{(B)} \rangle, \quad (2.4)$$

where $|e_i^{(A)}\rangle$ and $|e_j^{(B)}\rangle$ describe orthonormal bases for the Hilbert spaces \mathcal{H}_A and \mathcal{H}_B , respectively. The Rényi odd entropy of order n_o between the subsystems A and B may be defined as [45]

$$S_o^{(n_o)}(A:B) = \frac{1}{1-n_o} \log [\text{Tr}(\rho_{AB}^{T_B})^{n_o}], \quad (2.5)$$

where n_o is an odd integer. The OEE between the subsystems A and B may now be defined through the analytic continuation of the odd integer $n_o \rightarrow 1$ in Eq. (2.5) as follows [8]:

$$\begin{aligned} S_o(A:B) &= \lim_{n_o \rightarrow 1} [S_o^{(n_o)}(A:B)] \\ &= \lim_{n_o \rightarrow 1} \frac{1}{1-n_o} \log [\text{Tr}(\rho_{AB}^{T_B})^{n_o}]. \end{aligned} \quad (2.6)$$

C. Odd entanglement entropy in a CFT_2

The subsystems A and B in a CFT_2 may be characterized by the disjoint spatial intervals $[z_1, z_2]$ and $[z_3, z_4]$ in the complex plane [with $x_1 < x_2 < x_3 < x_4, x = \text{Re}(z)$]. In [8] the author advanced a replica technique to compute the OEE for bipartite systems in a CFT_2 . The replica construction involves an n_o sheeted Riemann surface \mathcal{M}_{n_o} (where $n_o \in 2\mathbb{Z}^+ - 1$) prepared through the cyclic and anticyclic sewing of the branch cuts of n_o copies of the original manifold \mathcal{M} along the subsystems A and B respectively. Utilizing the replica technique, the trace of the partial transpose in Eq. (2.5) may be expressed in terms of the partition function on the n_o sheeted replica manifold as follows [46,47]:

$$\text{Tr}(\rho_{AB}^{T_B})^{n_o} = \frac{\mathbb{Z}[\mathcal{M}_{n_o}]}{(\mathbb{Z}[\mathcal{M}])^{n_o}}. \quad (2.7)$$

The relation in Eq. (2.7) may be utilized along with Eq. (2.6) to express the OEE in terms of the partition functions as follows:

$$S_o(A:B) = \lim_{n_o \rightarrow 1} \frac{1}{1-n_o} \log \left[\frac{\mathbb{Z}[\mathcal{M}_{n_o}]}{(\mathbb{Z}[\mathcal{M}])^{n_o}} \right]. \quad (2.8)$$

The partition function in Eq. (2.7) may be expressed in terms of an appropriate four-point correlation function of the twist and antitwist operators σ_{n_o} and $\bar{\sigma}_{n_o}$ located at the end points of the subsystems A and B as follows [46,47]:

$$\begin{aligned} &\frac{\mathbb{Z}[\mathcal{M}_{n_o}]}{(\mathbb{Z}[\mathcal{M}])^{n_o}} \\ &= \langle \sigma_{n_o}(z_1, \bar{z}_1) \bar{\sigma}_{n_o}(z_2, \bar{z}_2) \bar{\sigma}_{n_o}(z_3, \bar{z}_3) \sigma_{n_o}(z_4, \bar{z}_4) \rangle. \end{aligned} \quad (2.9)$$

We are now in a position to express the OEE between the subsystems A and B in terms of the four-point twist

correlator by combining Eqs. (2.5)–(2.7), and (2.9) as follows [8,46,47]:

$$\begin{aligned} S_o(A:B) &= \lim_{n_o \rightarrow 1} \frac{1}{1-n_o} \log [\langle \sigma_{n_o}(z_1, \bar{z}_1) \bar{\sigma}_{n_o}(z_2, \bar{z}_2) \\ &\quad \times \bar{\sigma}_{n_o}(z_3, \bar{z}_3) \sigma_{n_o}(z_4, \bar{z}_4) \rangle]. \end{aligned} \quad (2.10)$$

Note that σ_{n_o} and $\bar{\sigma}_{n_o}$ represent primary operators in CFT_2 with the following conformal dimensions [46–48]:

$$h_{n_o} = \bar{h}_{n_o} = \frac{c}{24} \left(n_o - \frac{1}{n_o} \right). \quad (2.11)$$

We also note in passing the conformal dimensions of the twist operators $\sigma_{n_o}^2$ and $\bar{\sigma}_{n_o}^2$, which are given as follows [8,46–48]:

$$h_{n_o}^{(2)} = \bar{h}_{n_o}^{(2)} = h_{n_o} = \frac{c}{24} \left(n_o - \frac{1}{n_o} \right). \quad (2.12)$$

D. Holographic odd entanglement entropy

We now follow [8,49] to present a brief review of the EWCS. Let M be any specific time slice of a bulk static AdS geometry in the context of $\text{AdS}_{d+1}/\text{CFT}_d$ framework. Consider a region A in ∂M . The entanglement wedge of A is given by the bulk region bounded by $A \cup \Gamma_A^{\min}$, where Γ_A^{\min} is the RT surface for A . It has been proposed to be dual to the reduced density matrix ρ_A [50–52]. To define the EWCS, we subdivide $A = A_1 \cup A_2$. A cross section of the entanglement wedge for $A_1 \cup A_2$, denoted by $\Sigma_{A_1 A_2}$, is defined such that it divides the wedge into two parts containing A and B separately. The EWCS between the subsystems A_1 and A_2 may then be defined as [53]

$$E_W(A_1 : A_2) = \frac{\text{Area}(\Sigma_{A_1 A_2}^{\min})}{4G_N}, \quad (2.13)$$

where $\Sigma_{A_1 A_2}^{\min}$ represents the minimal cross section of the entanglement wedge.

In [8] the author proposed a holographic duality describing the difference of the OEE and the EE in terms of the bulk EWCS of the bipartite state in question as follows:

$$S_o(A_1 : A_2) - S(A_1 \cup A_2) = E_W(A_1 : A_2), \quad (2.14)$$

where $S(A_1 \cup A_2)$ is the EE for the subsystem $A_1 \cup A_2$, and $E_W(A_1 : A_2)$ represents the EWCS between the subsystems A_1 and A_2 , respectively.

III. OEE IN A $\overline{\text{T}\overline{\text{T}}}$ DEFORMED CFT_2

In this section we develop an appropriate replica technique similar to those described in [32,34,42] for the computation of the OEE for various bipartite mixed-state

configurations in a $T\bar{T}$ deformed CFT_2 . To this end we consider two spatial intervals A and B in a $T\bar{T}$ deformed CFT_2 defined on a manifold \mathcal{M} . The partition functions on \mathcal{M} and \mathcal{M}_{n_o} for this deformed theory may be expressed in the path integral representation as follows [refer to Eq. (2.3)]

$$\begin{aligned} \mathbb{Z}[\mathcal{M}] &= \int_{\mathcal{M}} \mathcal{D}\phi e^{-\mathcal{I}_{\text{QFT}}^{(\mu)}[\phi]}, \\ \mathbb{Z}[\mathcal{M}_{n_o}] &= \int_{\mathcal{M}_{n_o}} \mathcal{D}\phi e^{-\mathcal{I}_{\text{QFT}}^{(\mu)}[\phi]}. \end{aligned} \quad (3.1)$$

When the deformation parameter μ is small, Eqs. (2.3), (2.8), and (3.1) may be utilized to express the OEE as

$$\begin{aligned} S_o^{(\mu)}(A:B) &= \lim_{n_o \rightarrow 1} \frac{1}{1 - n_o} \log \left[\frac{\int_{\mathcal{M}_{n_o}} \mathcal{D}\phi e^{-\mathcal{I}_{\text{CFT}} - \mu \int_{\mathcal{M}_{n_o}} (T\bar{T})}}{\left(\int_{\mathcal{M}} \mathcal{D}\phi e^{-\mathcal{I}_{\text{CFT}} - \mu \int_{\mathcal{M}} (T\bar{T})} \right)^{n_o}} \right], \end{aligned} \quad (3.2)$$

where the superscript μ has been used to specify the OEE in the deformed CFT_2 . The exponential factors in Eq. (3.2) may be further expanded for small μ to arrive at

$$\begin{aligned} S_o^{(\mu)}(A:B) &= \lim_{n_o \rightarrow 1} \frac{1}{1 - n_o} \log \left[\frac{\int_{\mathcal{M}_{n_o}} \mathcal{D}\phi e^{-\mathcal{I}_{\text{CFT}} (1 - \mu \int_{\mathcal{M}_{n_o}} (T\bar{T}) + \mathcal{O}(\mu^2))}}{\left[\int_{\mathcal{M}} \mathcal{D}\phi e^{-\mathcal{I}_{\text{CFT}} (1 - \mu \int_{\mathcal{M}} (T\bar{T}) + \mathcal{O}(\mu^2))} \right]^{n_o}} \right] \\ &= S_o^{(\text{CFT})}(A:B) + \lim_{n_o \rightarrow 1} \frac{1}{1 - n_o} \log \left[\frac{(1 - \mu \int_{\mathcal{M}_{n_o}} \langle T\bar{T} \rangle_{\mathcal{M}_{n_o}})}{(1 - \mu \int_{\mathcal{M}} \langle T\bar{T} \rangle_{\mathcal{M}})^{n_o}} \right]. \end{aligned} \quad (3.3)$$

The term $S_o^{(\text{CFT})}(A:B) \equiv S_o^{(\mu=0)}(A:B)$ in Eq. (3.3) represents the corresponding OEE for the undeformed CFT_2 . The expectation values of the $T\bar{T}$ operator on the manifolds \mathcal{M} and \mathcal{M}_{n_o} appearing in Eq. (3.3) are defined as follows:

$$\langle T\bar{T} \rangle_{\mathcal{M}} = \frac{\int_{\mathcal{M}} \mathcal{D}\phi e^{-\mathcal{I}_{\text{CFT}}(T\bar{T})}}{\int_{\mathcal{M}} \mathcal{D}\phi e^{-\mathcal{I}_{\text{CFT}}}}, \quad \langle T\bar{T} \rangle_{\mathcal{M}_{n_o}} = \frac{\int_{\mathcal{M}_{n_o}} \mathcal{D}\phi e^{-\mathcal{I}_{\text{CFT}}(T\bar{T})}}{\int_{\mathcal{M}_{n_o}} \mathcal{D}\phi e^{-\mathcal{I}_{\text{CFT}}}}. \quad (3.4)$$

The second term on the right-hand side of Eq. (3.3) may be simplified to obtain the first-order correction in μ to the OEE due to the $T\bar{T}$ deformation as follows:

$$\delta S_o(A:B) = -\mu \lim_{n_o \rightarrow 1} \frac{1}{1 - n_o} \left[\int_{\mathcal{M}_{n_o}} \langle T\bar{T} \rangle_{\mathcal{M}_{n_o}} - n_o \int_{\mathcal{M}} \langle T\bar{T} \rangle_{\mathcal{M}} \right]. \quad (3.5)$$

IV. $T\bar{T}$ DEFORMED THERMAL CFT_2 AND HOLOGRAPHY

A. OEE in a $T\bar{T}$ deformed thermal CFT_2

We now investigate the behavior of the deformed CFT_2 at a finite temperature $1/\beta$. The corresponding manifold \mathcal{M} for this configuration is given by an infinitely long cylinder of circumference β with the Euclidean time direction compactified by the periodic identification $\tau \sim \tau + \beta$. This cylindrical manifold \mathcal{M} may be described by the complex coordinates [48]

$$w = x + i\tau, \quad \bar{w} = x - i\tau, \quad (4.1)$$

with the spatial coordinate $x \in (-\infty, \infty)$ and the time coordinate $\tau \in (0, \beta)$. The cylinder \mathcal{M} may be further expressed in terms of the complex plane \mathbb{C} through the following conformal map [48]

$$z = e^{\frac{2\pi w}{\beta}}, \quad \bar{z} = e^{\frac{2\pi \bar{w}}{\beta}}, \quad (4.2)$$

where (z, \bar{z}) represent the coordinates on the complex plane. The transformation of the stress tensors under the conformal map described in Eq. (4.2) is given as

$$\begin{aligned} T(w) &= \left(\frac{2\pi z}{\beta} \right)^2 T(z) - \frac{\pi^2 c}{6\beta^2}, \\ \bar{T}(\bar{w}) &= \left(\frac{2\pi \bar{z}}{\beta} \right)^2 \bar{T}(\bar{z}) - \frac{\pi^2 c}{6\beta^2}. \end{aligned} \quad (4.3)$$

The relations in Eq. (4.3) may be utilized to arrive at

$$\langle T(w)\bar{T}(\bar{w}) \rangle_{\mathcal{M}} = \left(\frac{\pi^2 c}{6\beta^2} \right)^2, \quad (4.4)$$

where we have used the fact that $\langle T(z) \rangle_{\mathbb{C}} = \langle \bar{T}(\bar{z}) \rangle_{\mathbb{C}} = 0$ for the vacuum state of an undeformed CFT_2 described by the complex plane. In the following subsections, we utilize Eq. (3.5) to compute the first-order correction in μ to the

OEE in a finite temperature $T\bar{T}$ deformed CFT_2 for two disjoint intervals, two adjacent intervals, and a single interval.

1. Two disjoint intervals

We begin with the bipartite mixed-state configuration of two disjoint spatial intervals $A = [x_1, x_2]$ and $B = [x_3, x_4]$

in a $T\bar{T}$ deformed CFT_2 at a finite temperature $1/\beta$, defined on the cylindrical manifold \mathcal{M} ($x_1 < x_2 < x_3 < x_4$). Note that the intervals may also be represented as $A = [w_1, w_2]$ and $B = [w_3, w_4]$ with $\tau = 0$ [cf. Eq. (4.1)]. The value of $\langle T\bar{T} \rangle_{\mathcal{M}_{n_o}}$ on the replica manifold \mathcal{M}_{n_o} may be computed by insertion of the $T\bar{T}$ operator into the appropriate four-point twist correlator as follows [54,55]:

$$\begin{aligned} \int_{\mathcal{M}_{n_o}} \langle T\bar{T} \rangle_{\mathcal{M}_{n_o}} &= \sum_{k=1}^{n_o} \int_{\mathcal{M}} \frac{\langle T_k(w) \bar{T}_k(\bar{w}) \sigma_{n_o}(w_1, \bar{w}_1) \bar{\sigma}_{n_o}(w_2, \bar{w}_2) \bar{\sigma}_{n_o}(w_3, \bar{w}_3) \sigma_{n_o}(w_4, \bar{w}_4) \rangle_{\mathcal{M}}}{\langle \sigma_{n_o}(w_1, \bar{w}_1) \bar{\sigma}_{n_o}(w_2, \bar{w}_2) \bar{\sigma}_{n_o}(w_3, \bar{w}_3) \sigma_{n_o}(w_4, \bar{w}_4) \rangle_{\mathcal{M}}} \\ &= \int_{\mathcal{M}} \frac{1}{n_o} \frac{\langle T^{(n_o)}(w) \bar{T}^{(n_o)}(\bar{w}) \sigma_{n_o}(w_1, \bar{w}_1) \bar{\sigma}_{n_o}(w_2, \bar{w}_2) \bar{\sigma}_{n_o}(w_3, \bar{w}_3) \sigma_{n_o}(w_4, \bar{w}_4) \rangle_{\mathcal{M}}}{\langle \sigma_{n_o}(w_1, \bar{w}_1) \bar{\sigma}_{n_o}(w_2, \bar{w}_2) \bar{\sigma}_{n_o}(w_3, \bar{w}_3) \sigma_{n_o}(w_4, \bar{w}_4) \rangle_{\mathcal{M}}}. \end{aligned} \quad (4.5)$$

Here $T_k(w)$ and $\bar{T}_k(\bar{w})$ are the stress tensors of the undeformed CFT_2 on the k th sheet of the Riemann surface \mathcal{M}_{n_o} , while $T^{(n_o)}(w)$, $\bar{T}^{(n_o)}(\bar{w})$ represent the stress tensors on \mathcal{M}_{n_o} [54,55]. $\sigma_{n_o}(w_i, \bar{w}_i)$, $\bar{\sigma}_{n_o}(w_i, \bar{w}_i)$ represent the twist operators located at the end points w_i of the intervals. An identity described in [34] has been used to derive the last line of Eq. (4.5). The relation in Eq. (4.3) may now be utilized to transform the stress tensors from the cylindrical manifold to the complex plane. The following Ward identities are then employed to express the correlation functions involving the stress tensors in terms of the twist correlators on the complex plane

$$\begin{aligned} \langle T^{(n_o)}(z) \mathcal{O}_1(z_1, \bar{z}_1) \dots \mathcal{O}_m(z_m, \bar{z}_m) \rangle_{\mathbb{C}} &= \sum_{j=1}^m \left(\frac{h_j}{(z - z_j)^2} + \frac{1}{(z - z_j)} \partial_{z_j} \right) \langle \mathcal{O}_1(z_1, \bar{z}_1) \dots \mathcal{O}_m(z_m, \bar{z}_m) \rangle_{\mathbb{C}}, \\ \langle \bar{T}^{(n_o)}(\bar{z}) \mathcal{O}_1(z_1, \bar{z}_1) \dots \mathcal{O}_m(z_m, \bar{z}_m) \rangle_{\mathbb{C}} &= \sum_{j=1}^m \left(\frac{\bar{h}_j}{(\bar{z} - \bar{z}_j)^2} + \frac{1}{(\bar{z} - \bar{z}_j)} \partial_{\bar{z}_j} \right) \langle \mathcal{O}_1(z_1, \bar{z}_1) \dots \mathcal{O}_m(z_m, \bar{z}_m) \rangle_{\mathbb{C}}, \end{aligned} \quad (4.6)$$

where \mathcal{O}_i s represent arbitrary primary operators with conformal dimensions (h_i, \bar{h}_i) . Utilizing Eq. (4.3), we may now express the expectation value in Eq. (4.5) as

$$\begin{aligned} \int_{\mathcal{M}_{n_o}} \langle T\bar{T} \rangle_{\mathcal{M}_{n_o}} &= \frac{1}{n_o} \int_{\mathcal{M}} \frac{1}{\langle \sigma_{n_o}(z_1, \bar{z}_1) \bar{\sigma}_{n_o}(z_2, \bar{z}_2) \bar{\sigma}_{n_o}(z_3, \bar{z}_3) \sigma_{n_o}(z_4, \bar{z}_4) \rangle_{\mathbb{C}}} \left[-\frac{\pi^2 c n_o}{6\beta^2} + \left(\frac{2\pi z}{\beta} \right)^2 \sum_{j=1}^4 \left(\frac{h_j}{(z - z_j)^2} + \frac{1}{(z - z_j)} \partial_{z_j} \right) \right] \\ &\times \left[-\frac{\pi^2 c n_o}{6\beta^2} + \left(\frac{2\pi \bar{z}}{\beta} \right)^2 \sum_{k=1}^4 \left(\frac{\bar{h}_k}{(\bar{z} - \bar{z}_k)^2} + \frac{1}{(\bar{z} - \bar{z}_k)} \partial_{\bar{z}_k} \right) \right] \langle \sigma_{n_o}(z_1, \bar{z}_1) \bar{\sigma}_{n_o}(z_2, \bar{z}_2) \bar{\sigma}_{n_o}(z_3, \bar{z}_3) \sigma_{n_o}(z_4, \bar{z}_4) \rangle_{\mathbb{C}}, \end{aligned} \quad (4.7)$$

where $h_i = \bar{h}_i = h_{n_o}$ ($i = 1, 2, 3, 4$) [see Eq. (2.11)]. The four-point twist correlator in Eq. (4.7) for two disjoint intervals in proximity described by the t -channel is given by [8,56]

$$\langle \sigma_{n_o}(z_1, \bar{z}_1) \bar{\sigma}_{n_o}(z_2, \bar{z}_2) \bar{\sigma}_{n_o}(z_3, \bar{z}_3) \sigma_{n_o}(z_4, \bar{z}_4) \rangle_{\mathbb{C}} \approx |z_{14} z_{23}|^{-4h_{n_o}} \left(\frac{1 + \sqrt{\eta}}{1 - \sqrt{\eta}} \right)^{-h_{n_o}^{(2)}} \left(\frac{1 + \sqrt{\eta}}{1 - \sqrt{\eta}} \right)^{-\bar{h}_{n_o}^{(2)}}. \quad (4.8)$$

The conformal dimensions h_{n_o} , $h_{n_o}^{(2)}$, and $\bar{h}_{n_o}^{(2)}$ in Eq. (4.8) are given in Eqs. (2.11) and (2.12). We have defined the cross ratio $\eta := \frac{z_{12} z_{34}}{z_{13} z_{24}}$ where $z_{ij} \equiv z_i - z_j$.

We are now in a position to obtain the first-order correction due to μ in the OEE of two disjoint intervals in a $T\bar{T}$ deformed finite temperature CFT_2 by substituting Eqs. (4.4), (4.7), and (4.8) into Eq. (3.5) as follows:

$$\begin{aligned} \delta S_o(A:B) = & -\frac{\mu c^2 \pi^4 \sqrt{\eta}}{18\beta^4 z_{21} z_{32} z_{41} z_{43}} \int_{\mathcal{M}} z^2 \left[\frac{z_{32} z_{42} [z_{31} (2z - 3z_1 + z_4) \sqrt{\eta} + z_{43} (z - z_1)]}{(z - z_1)^2} \right. \\ & + \frac{z_{31} z_{41} [z_{42} (2z - 3z_2 + z_3) \sqrt{\eta} - z_{43} (z - z_2)]}{(z - z_2)^2} - \frac{z_{42} z_{41} [z_{31} (2z + z_2 - 3z_3) \sqrt{\eta} - z_{21} (z - z_3)]}{(z - z_3)^2} \\ & \left. - \frac{z_{31} z_{32} [z_{42} (2z + z_1 - 3z_4) \sqrt{\eta} + z_{21} (z - z_4)]}{(z - z_4)^2} \right] + \text{H.c.} \end{aligned} \quad (4.9)$$

The detailed derivation of the definite integrals in Eq. (4.9) has been provided in Appendix A 1. These results may be used to arrive at

$$\begin{aligned} \delta S_o(A:B) = & \frac{\mu c^2 \pi^3}{36\beta^2} \left[\frac{\left\{ \left(\sqrt{\frac{z_{42} z_{43}}{z_{21} z_{31}}} + 1 \right) z_1 + z_4 \right\}}{z_{41}} \log \left[\frac{z_1}{z_2} \right] + \frac{\left(\sqrt{\frac{z_{21} z_{43}}{z_{31} z_{42}}} - 2 \right) (z_1 z_2 - z_3 z_4)}{z_{32} z_{41}} \log \left[\frac{z_2}{z_3} \right] \right. \\ & \left. + \frac{\left\{ z_1 - \left(\sqrt{\frac{z_{21} z_{31}}{z_{42} z_{43}}} - 1 \right) z_4 \right\}}{z_{41}} \log \left[\frac{z_3}{z_4} \right] + \text{H.c.} \right]. \end{aligned} \quad (4.10)$$

We may now substitute $z_i = \bar{z}_i = e^{\frac{2\pi x_i}{\beta}}$ (at $\tau_i = 0$) into Eq. (4.10) to finally obtain the leading-order corrections to the OEE as follows:

$$\begin{aligned} \delta S_o(A:B) = & -\frac{\mu c^2 \pi^4}{9\beta^3} \sqrt{\frac{\sinh\left(\frac{\pi x_{21}}{\beta}\right) \sinh\left(\frac{\pi x_{43}}{\beta}\right)}{\sinh\left(\frac{\pi x_{31}}{\beta}\right) \sinh\left(\frac{\pi x_{42}}{\beta}\right)}} \left[x_{21} \coth\left(\frac{\pi x_{21}}{\beta}\right) - x_{32} \coth\left(\frac{\pi x_{32}}{\beta}\right) - x_{41} \coth\left(\frac{\pi x_{41}}{\beta}\right) + x_{43} \coth\left(\frac{\pi x_{43}}{\beta}\right) \right] \\ & - \frac{\mu c^2 \pi^4}{9\beta^3} \left[x_{32} \coth\left(\frac{\pi x_{32}}{\beta}\right) + x_{41} \coth\left(\frac{\pi x_{41}}{\beta}\right) \right], \end{aligned} \quad (4.11)$$

where $x_{ij} \equiv x_i - x_j$. It is worth noting that the last term in the above expression is nothing but the leading-order corrections to the entanglement entropy of the two disjoint intervals in the t -channel. Remarkably, in the low-temperature limit $\beta \gg x_{ij}$, the corrections to the OEE scales exactly like that for the entanglement entropy, $\frac{-2\mu\pi^3 c^2}{9\beta^2}$ [32]. In particular, in the zero-temperature limit $\beta \rightarrow \infty$, the corrections vanish conforming to our expectations.

2. Two adjacent intervals

We now turn our attention to the bipartite mixed state configuration of two adjacent intervals $A = [x_1, x_2]$ and $B = [x_2, x_3]$ in a $T\bar{T}$ deformed CFT_2 at a finite temperature $1/\beta$ ($x_1 < x_2 < x_3$). As earlier the intervals may be expressed as $A = [w_1, w_2]$ and $B = [w_2, w_3]$ with $\tau = 0$. The value of $\langle T\bar{T} \rangle_{\mathcal{M}_{n_o}}$ for two adjacent intervals may be evaluated in a manner similar to that of two disjoint intervals as follows:

$$\int_{\mathcal{M}_{n_o}} \langle T\bar{T} \rangle_{\mathcal{M}_{n_o}} = \int_{\mathcal{M}} \frac{1}{n_o} \frac{\langle T^{(n_o)}(w) \bar{T}^{(n_o)}(\bar{w}) \sigma_{n_o}(w_1, \bar{w}_1) \bar{\sigma}_{n_o}^2(w_2, \bar{w}_2) \sigma_{n_o}(w_3, \bar{w}_3) \rangle_{\mathcal{M}}}{\langle \sigma_{n_o}(w_1, \bar{w}_1) \bar{\sigma}_{n_o}^2(w_2, \bar{w}_2) \sigma_{n_o}(w_3, \bar{w}_3) \rangle_{\mathcal{M}}}. \quad (4.12)$$

As before the relations in Eqs. (4.3) and (4.6) may be utilized to express the expectation value in Eq. (4.12) as follows:

$$\begin{aligned} \int_{\mathcal{M}_{n_o}} \langle T\bar{T} \rangle_{\mathcal{M}_{n_o}} = & \frac{1}{n_o} \int_{\mathcal{M}} \frac{1}{\langle \sigma_{n_o}(z_1, \bar{z}_1) \bar{\sigma}_{n_o}^2(z_2, \bar{z}_2) \sigma_{n_o}(z_3, \bar{z}_3) \rangle_{\mathcal{C}}} \left[-\frac{\pi^2 c n_o}{6\beta^2} + \left(\frac{2\pi z}{\beta} \right)^2 \sum_{j=1}^3 \left(\frac{h_j}{(z - z_j)^2} + \frac{1}{(z - z_j)} \partial_{z_j} \right) \right] \\ & \times \left[-\frac{\pi^2 c n_o}{6\beta^2} + \left(\frac{2\pi \bar{z}}{\beta} \right)^2 \sum_{k=1}^3 \left(\frac{\bar{h}_k}{(\bar{z} - \bar{z}_k)^2} + \frac{1}{(\bar{z} - \bar{z}_k)} \partial_{\bar{z}_k} \right) \right] \langle \sigma_{n_o}(z_1, \bar{z}_1) \bar{\sigma}_{n_o}^2(z_2, \bar{z}_2) \sigma_{n_o}(z_3, \bar{z}_3) \rangle_{\mathcal{C}}. \end{aligned} \quad (4.13)$$

In eq. (4.13) we have $h_1 = h_3 = h_{n_o}, h_2 = h_{n_o}^{(2)}$ with $\bar{h}_i = h_i$ ($i = 1, 2, 3$) [see Eq. (2.11)]. The three-point twist correlator in Eq. (4.13) is given by [57]

$$\langle \sigma_{n_o}(z_1, \bar{z}_1) \bar{\sigma}_{n_o}^2(z_2, \bar{z}_2) \sigma_{n_o}(z_3, \bar{z}_3) \rangle_{\mathcal{C}} = \frac{\mathcal{C}_{\sigma_{n_o} \bar{\sigma}_{n_o}^2 \sigma_{n_o}}}{\left(\frac{h_{n_o}^{(2)} z_{12} h_{n_o}^{(2)} z_{23} 2h_{n_o} - h_{n_o}^{(2)}}{(z_{12} z_{23} z_{13})} \right) \left(\frac{\bar{h}_{n_o}^{(2)} \bar{z}_{12} \bar{h}_{n_o}^{(2)} 2\bar{h}_{n_o} - \bar{h}_{n_o}^{(2)}}{(\bar{z}_{12} \bar{z}_{23} \bar{z}_{13})} \right)}, \quad (4.14)$$

where $\mathcal{C}_{\sigma_{n_o} \bar{\sigma}_{n_o}^2 \sigma_{n_o}}$ is the relevant OPE coefficient. The first-order correction due to μ in the OEE of two adjacent intervals in a $T\bar{T}$ deformed thermal CFT_2 may now be obtained by substituting Eqs. (4.4), (4.13), and (4.14) into Eq. (3.5) as follows:

$$\delta S_o(A:B) = -\frac{\mu c^2 \pi^4}{18\beta^4} \int_{\mathcal{M}} z^2 \left[\frac{1}{(z-z_1)^2} + \frac{1}{(z-z_2)^2} + \frac{1}{(z-z_3)^2} + \frac{(-3z+z_1+z_2+z_3)}{(z-z_1)(z-z_2)(z-z_3)} + \text{H.c.} \right]. \quad (4.15)$$

The technical details of the definite integrals in Eq. (4.15) have been included in Appendix A 2. The correction to the OEE may then be expressed as

$$\delta S_o(A:B) = -\frac{\mu c^2 \pi^3}{36\beta^2} \left[\frac{(z_1^2 - z_2 z_3) \log(\frac{z_1}{z_2})}{z_{12} z_{13}} + \frac{(z_1 z_2 - z_3^2) \log(\frac{z_2}{z_3})}{z_{23} z_{13}} + \text{H.c.} \right]. \quad (4.16)$$

As earlier we may now restore the x coordinates by inserting $z_i = \bar{z}_i = e^{\frac{2\pi x_i}{\beta}}$ (at $\tau_i = 0$) into Eq. (4.16) to arrive at

$$\delta S_o(A:B) = -\left(\frac{\mu c^2 \pi^4}{36\beta^3} \right) \frac{x_{21} \cosh(\frac{2\pi x_{21}}{\beta}) + x_{32} \cosh(\frac{2\pi x_{32}}{\beta}) - x_{31} \cosh(\frac{2\pi x_{31}}{\beta})}{\sinh(\frac{\pi x_{21}}{\beta}) \sinh(\frac{\pi x_{32}}{\beta}) \sinh(\frac{\pi x_{31}}{\beta})}. \quad (4.17)$$

Once again, we see that the leading-order corrections to the OEE scales exactly like that of the entanglement entropy in the low-temperature limit $\beta \gg x_{ij}$. It is interesting to note that we are unable to reproduce the above result by taking an appropriate adjacent limit of the corrections to the disjoint intervals given in Eq. (4.11). However, this does not lead to any contradiction since our field theory results are perturbative and there is no *a priori* reason to believe that a limiting analysis holds in each order of conformal perturbation theory. More evidence towards this mismatch will be provided from a holographic viewpoint in Sec. IV B 2.

3. A single interval

We finally focus on the case of a single interval $A = [-\ell, 0]$ in a thermal $T\bar{T}$ deformed CFT_2 ($\ell > 0$). To this end

it is required to consider two auxiliary intervals $B_1 = [-L, -\ell]$ and $B_2 = [0, L]$ on either side of the interval A with $B \equiv B_1 \cup B_2$ ($L \gg \ell$) [48]. The intervals may be equivalently represented by the coordinates $B_1 = [x_1, x_2]$, $A = [x_2, x_3]$ and $B_2 = [x_3, x_4]$, with $x_1 = -L, x_2 = -\ell, x_3 = 0, x_4 = L$ and $x_1 < x_2 < x_3 < x_4$. As before the intervals may also be characterized as $B_1 = [w_1, w_2]$, $A = [w_2, w_3]$, and $B_2 = [w_3, w_4]$ with $\tau = 0$. The OEE for the mixed-state configuration of the single interval A is then evaluated by implementing the bipartite limit $L \rightarrow \infty$ ($B_1 \cup B_2 \rightarrow A^c$) subsequent to the replica limit $n_o \rightarrow 1$ [48]. For the configuration described above, the integral of $\langle T\bar{T} \rangle_{\mathcal{M}_{n_o}}$ on the replica manifold is given by

$$\int_{\mathcal{M}_{n_o}} \langle T\bar{T} \rangle_{\mathcal{M}_{n_o}} = \int_{\mathcal{M}} \frac{1}{n_o} \frac{\langle T^{(n_o)}(w) \bar{T}^{(n_o)}(\bar{w}) \sigma_{n_o}(w_1, \bar{w}_1) \bar{\sigma}_{n_o}^2(w_2, \bar{w}_2) \sigma_{n_o}^2(w_3, \bar{w}_3) \bar{\sigma}_{n_o}(w_4, \bar{w}_4) \rangle}{\langle \sigma_{n_o}(w_1, \bar{w}_1) \bar{\sigma}_{n_o}^2(w_2, \bar{w}_2) \sigma_{n_o}^2(w_3, \bar{w}_3) \bar{\sigma}_{n_o}(w_4, \bar{w}_4) \rangle}. \quad (4.18)$$

As earlier Eq. (4.18) may be simplified by utilizing Eqs. (4.3) and (4.6) as follows:

$$\begin{aligned} \int_{\mathcal{M}_{n_o}} \langle T\bar{T} \rangle_{\mathcal{M}_{n_o}} &= \frac{1}{n_o} \int_{\mathcal{M}} \frac{1}{\langle \sigma_{n_o}(z_1, \bar{z}_1) \bar{\sigma}_{n_o}^2(z_2, \bar{z}_2) \sigma_{n_o}^2(z_3, \bar{z}_3) \bar{\sigma}_{n_o}(z_4, \bar{z}_4) \rangle} \left[-\frac{\pi^2 c n_o}{6\beta^2} + \left(\frac{2\pi z}{\beta} \right)^2 \sum_{j=1}^4 \left(\frac{h_j}{(z-z_j)^2} + \frac{1}{(z-z_j)} \partial_{z_j} \right) \right] \\ &\times \left[-\frac{\pi^2 c n_o}{6\beta^2} + \left(\frac{2\pi \bar{z}}{\beta} \right)^2 \sum_{k=1}^4 \left(\frac{\bar{h}_k}{(\bar{z}-\bar{z}_k)^2} + \frac{1}{(\bar{z}-\bar{z}_k)} \partial_{\bar{z}_k} \right) \right] \langle \sigma_{n_o}(z_1, \bar{z}_1) \bar{\sigma}_{n_o}^2(z_2, \bar{z}_2) \sigma_{n_o}^2(z_3, \bar{z}_3) \bar{\sigma}_{n_o}(z_4, \bar{z}_4) \rangle_{\mathcal{C}}, \quad (4.19) \end{aligned}$$

where $h_1 = h_4 = h_{n_o}$, $h_2 = h_3 = h_{n_o}^{(2)}$ with $\bar{h}_i = h_i$ ($i = 1, 2, 3, 4$) [see Eqs. (2.11) and (2.12)]. The four-point twist correlator in Eq. (4.19) is given by [48]

$$\langle \sigma_{n_o}(z_1, \bar{z}_1) \bar{\sigma}_{n_o}^2(z_2, \bar{z}_2) \sigma_{n_o}^2(z_3, \bar{z}_3) \bar{\sigma}_{n_o}(z_4, \bar{z}_4) \rangle = c_{n_o} c_{n_o}^{(2)} \left(\frac{\mathcal{F}_{n_o}(\eta)}{z_{14}^{2h_{n_o}} z_{23}^{2h_{n_o}^{(2)}} \eta^{h_{n_o}^{(2)}}} \right) \left(\frac{\bar{\mathcal{F}}_{n_o}(\bar{\eta})}{\bar{z}_{14}^{2\bar{h}_{n_o}} \bar{z}_{23}^{2\bar{h}_{n_o}^{(2)}} \bar{\eta}^{h_{n_o}^{(2)}}} \right), \quad (4.20)$$

where c_{n_o} and $c_{n_o}^{(2)}$ are the normalization constants. The functions $\mathcal{F}_{n_o}(\eta)$ and $\bar{\mathcal{F}}_{n_o}(\bar{\eta})$ in Eq. (4.20) satisfy the following OPE limits:

$$\mathcal{F}_{n_o}(1) \bar{\mathcal{F}}_{n_o}(1) = 1, \quad \mathcal{F}_{n_o}(0) \bar{\mathcal{F}}_{n_o}(0) = \frac{\mathcal{C}_{\sigma_{n_o} \bar{\sigma}_{n_o}^2 \bar{\sigma}_{n_o}}}{c_{n_o}^{(2)}},$$

where $\mathcal{C}_{\sigma_{n_o} \bar{\sigma}_{n_o}^2 \bar{\sigma}_{n_o}}$ represents the relevant OPE coefficient. As earlier, Eqs. (4.4), (4.19), and (4.20) may be substituted into Eq. (3.5) to arrive at

$$\delta S_o(A:B) = -\frac{\mu c^2 \pi^4}{18\beta^4} \int_{\mathcal{M}} \left[\sum_{j=1}^4 \frac{z^2}{(z-z_j)^2} - \sum_{j=1}^4 \frac{\bar{z}^2}{(\bar{z}-\bar{z}_j)^2} \right] \partial_{z_j} (\log[z_{23}^2 z_{14}^2 \eta f(\eta)]) + \text{H.c.} \quad (4.21)$$

The functions $f(\eta)$ and $\bar{f}(\bar{\eta})$ introduced in Eq. (4.21) are defined as follows:

$$\lim_{n_o \rightarrow 1} [\mathcal{F}_{n_o}(\eta)]^{\frac{1}{1-n_o}} = [f(\eta)]^{c/12}, \quad \lim_{n_o \rightarrow 1} [\bar{\mathcal{F}}_{n_o}(\bar{\eta})]^{\frac{1}{1-n_o}} = [\bar{f}(\bar{\eta})]^{c/12}.$$

The first-order correction due to μ in the OEE of a single interval in a $\text{T}\bar{\text{T}}$ deformed CFT_2 at a finite temperature $1/\beta$ may now be computed from Eq. (4.21) by reverting back to the coordinates involving ℓ , L and implementing the bipartite limit $L \rightarrow \infty$ as follows:

$$\delta S_o(A:A^c) = -\frac{2\mu c^2 \pi^4 \ell}{9\beta^3} \left(\frac{1}{e^{\frac{2\pi\ell}{\beta}} - 1} - e^{-\frac{2\pi\ell}{\beta}} \frac{f'[e^{-\frac{2\pi\ell}{\beta}}]}{2f[e^{-\frac{2\pi\ell}{\beta}}]} \right) - \lim_{L \rightarrow \infty} \left[\frac{\mu c^2 \pi^4 L}{9\beta^3} \coth\left(\frac{2\pi L}{\beta}\right) \right]. \quad (4.22)$$

The technical details of the integrals necessary to arrive at Eq. (4.22) from Eq. (4.21) have been provided in Appendix A 3. Note that the second term on the right-hand side of Eq. (4.22) represents a divergent piece in the OEE for a single interval. Essentially, the quantity inside the parenthesis of the second term is the leading-order correction to the entanglement entropy of the interval $A \cup B_1 \cup B_2$. In the bipartite limit $L \rightarrow \infty$, this represents the entanglement entropy of the entire system and hence should be vanishing. The IR divergence is an artifact of placing a cutoff in a continuum field theory.²

Interestingly the universal finite piece of the OEE for a single interval in a $\text{T}\bar{\text{T}}$ -deformed CFT_2 may be rewritten up to leading order in the deformation as follows:

²Similar divergences are observed in the usual CFT_2 in its vacuum state. The entanglement entropy for a single interval of length ℓ at zero temperature is given by $\frac{\ell}{3} \log(\frac{\ell}{\epsilon})$ [54], which diverges logarithmically as $\ell \rightarrow \infty$.

$$S_o(A:A^c) = S_A - S_A^{\text{Th}}, \quad (4.23)$$

where the thermal entropy S_A^{Th} is now given by

$$S_A^{\text{Th}} = \frac{\pi c \ell}{3\beta} \left(1 - \mu \frac{\pi^3 c}{3\beta^2} \right). \quad (4.24)$$

A comparison of the above expression to the thermal contribution in the undeformed case, $\frac{\pi c \ell}{3\beta}$ [48], indicates that the thermal entropy receives nontrivial corrections due to the $\text{T}\bar{\text{T}}$ -deformation.

B. Holographic OEE in a $\text{T}\bar{\text{T}}$ deformed thermal CFT_2

We now turn our attention to the holographic description of the OEE as advanced in [8] for various bipartite mixed states in a $\text{T}\bar{\text{T}}$ deformed CFT_2 at a finite temperature $1/\beta$.

The holographic dual of a $T\bar{T}$ deformed CFT_2 is described by the bulk AdS_3 geometry corresponding to the undeformed CFT_2 with a finite cut-off radius r_c given as follows [20]:

$$r_c = \sqrt{\frac{6R^4}{\pi c\mu}} = \frac{R^2}{\epsilon}. \quad (4.25)$$

In Eq. (4.25) μ is the deformation parameter, c is the central charge, ϵ is the UV cutoff of the field theory, and R is the AdS_3 radius. For a $T\bar{T}$ deformed CFT_2 at a finite temperature $1/\beta$, the corresponding bulk dual is characterized by a BTZ black hole [58] with a finite cutoff, represented by [20]

$$ds^2 = -\frac{r^2 - r_h^2}{R^2} dt^2 + \frac{R^2}{r^2 - r_h^2} dr^2 + r^2 d\tilde{x}^2. \quad (4.26)$$

In the above metric, the horizon of the black hole is located at $r = r_h$, with $\beta = \frac{2\pi R^2}{r_h}$ as the inverse temperature of the black hole and the dual CFT_2 . For simplicity from now onwards we set the AdS radius $R = 1$. The metric on the $T\bar{T}$ deformed CFT_2 , located at the cutoff radius $r = r_c$, is conformal to the bulk metric at $r = r_c$ as follows [32,34]:

$$ds^2 = -dt^2 + \frac{d\tilde{x}^2}{1 - \frac{r_h^2}{r_c^2}} \equiv -dt^2 + dx^2, \quad x = \frac{r_c \tilde{x}}{\sqrt{r_c^2 - r_h^2}}, \quad (4.27)$$

where x represents the spatial coordinate on the deformed CFT_2 . To compute the EWCS, we embed the BTZ black hole described by Eq. (4.26) in $\mathbb{R}^{2,2}$ as follows [10]:

$$ds^2 = \eta_{AB} dX^A dX^B = -dX_0^2 - dX_1^2 + dX_2^2 + dX_3^2, \quad X^2 = -1. \quad (4.28)$$

The metric in Eq. (4.26) may then be described by these embedding coordinates as follows [59,60]:

$$\begin{aligned} X_0(t, r, x) &= \sqrt{\frac{r^2}{r_h^2} - 1} \sinh\left(\frac{2\pi t}{\beta}\right), \\ X_1(t, r, x) &= \frac{r}{r_h} \cosh\left(\frac{2\pi \tilde{x}}{\beta}\right), \\ X_2(t, r, x) &= \sqrt{\frac{r^2}{r_h^2} - 1} \cosh\left(\frac{2\pi t}{\beta}\right), \\ X_3(t, r, x) &= \frac{r}{r_h} \sinh\left(\frac{2\pi \tilde{x}}{\beta}\right). \end{aligned} \quad (4.29)$$

Note that for convenience the embedding coordinates in Eq. (4.29) are parametrized in terms of the coordinate x

described in Eq. (4.27). We also introduce a new coordinate $u = 1/r$ to simplify later calculations, with $u_c \equiv 1/r_c$ and $u_h \equiv 1/r_h$. We also note the Brown-Henneaux formula $G_N = 3/(2c)$ described in [61], which will be extensively used in later sections. In the following subsections we apply the methods described above to compute the holographic OEE from Eq. (2.14) for two disjoint intervals, two adjacent intervals, and a single interval in a $T\bar{T}$ deformed thermal holographic CFT_2 .

1. Two disjoint intervals

We begin with the two disjoint spatial intervals $A = [x_1, x_2]$ and $B = [x_3, x_4]$ with $x_1 < x_2 < x_3 < x_4$ as described in section 4.1.1. The setup has been shown in Fig. 1. The EWCS involving the bulk points $X(s_1), X(s_2), X(s_3)$, and $X(s_4)$ is given by [10]

$$E_W = \frac{1}{4G_N} \cosh^{-1}\left(\frac{1 + \sqrt{u}}{\sqrt{v}}\right), \quad (4.30)$$

where

$$u = \frac{\xi_{12}^{-1} \xi_{34}^{-1}}{\xi_{13}^{-1} \xi_{24}^{-1}}, \quad v = \frac{\xi_{14}^{-1} \xi_{23}^{-1}}{\xi_{13}^{-1} \xi_{24}^{-1}}, \quad \xi_{ij}^{-1} = -X(s_i) \cdot X(s_j). \quad (4.31)$$

The four points on the boundary may be expressed in the global coordinates as $X(0, r_c, x_i)$ for $i = 1, 2, 3, 4$. The corresponding EWCS may then be computed from Eq. (4.30) as

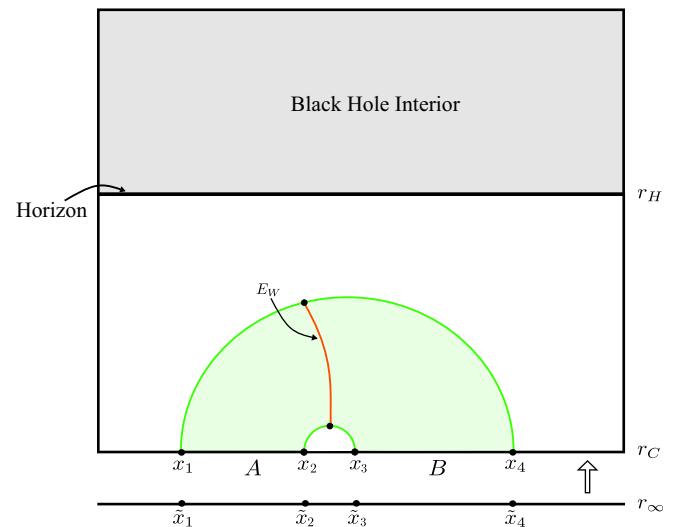


FIG. 1. EWCS for two disjoint intervals in a $T\bar{T}$ deformed thermal holographic CFT_2 . Figure based on [42].

$$\begin{aligned}
 E_W(A:B) = \frac{1}{4G_N} \cosh^{-1} & \left(\sqrt{\frac{\left[\frac{u_c^2 - u_h^2 + u_h^2 \cosh\left(\frac{\sqrt{u_h^2 - u_c^2} x_{31}}{u_h^2}\right) \right]}{u_c^2 - u_h^2 + u_h^2 \cosh\left(\frac{\sqrt{u_h^2 - u_c^2} x_{32}}{u_h^2}\right) \right]} \left[\frac{u_c^2 - u_h^2 + u_h^2 \cosh\left(\frac{\sqrt{u_h^2 - u_c^2} x_{42}}{u_h^2}\right) \right]}{u_c^2 - u_h^2 + u_h^2 \cosh\left(\frac{\sqrt{u_h^2 - u_c^2} x_{41}}{u_h^2}\right) \right]} \right. \\
 & \left. + \sqrt{\frac{\left[\frac{u_c^2 - u_h^2 + u_h^2 \cosh\left(\frac{\sqrt{u_h^2 - u_c^2} x_{21}}{u_h^2}\right) \right]}{u_c^2 - u_h^2 + u_h^2 \cosh\left(\frac{\sqrt{u_h^2 - u_c^2} x_{32}}{u_h^2}\right) \right]} \left[\frac{u_c^2 - u_h^2 + u_h^2 \cosh\left(\frac{\sqrt{u_h^2 - u_c^2} x_{43}}{u_h^2}\right) \right]}{u_c^2 - u_h^2 + u_h^2 \cosh\left(\frac{\sqrt{u_h^2 - u_c^2} x_{41}}{u_h^2}\right) \right]} \right). \quad (4.32)
 \end{aligned}$$

To compare with the field theory computations in Sec. IV A 1, we have to take the limit of small deformation parameter μ , corresponding to large cutoff radius r_c (or small u_c) [see Eq. (4.25)]. Further we must consider the high-temperature limit $\beta \ll |x_{ij}|$, as the dual cutoff geometry resembles a BTZ black hole only in the high-temperature limit. Expanding Eq. (4.32) for small u_c and $\beta \ll |x_{ij}|$ we arrive at

$$\begin{aligned}
 E_W(A:B) = \frac{1}{4G_N} \cosh^{-1} & \left[1 + 2 \frac{\sinh\left(\frac{x_{21}}{2u_h}\right) \sinh\left(\frac{x_{43}}{2u_h}\right)}{\sinh\left(\frac{x_{32}}{2u_h}\right) \sinh\left(\frac{x_{41}}{2u_h}\right)} \right] \\
 & - \frac{u_c^2}{16G_N u_h^3} \sqrt{\frac{\sinh\left(\frac{x_{21}}{2u_h}\right) \sinh\left(\frac{x_{43}}{2u_h}\right)}{\sinh\left(\frac{x_{31}}{2u_h}\right) \sinh\left(\frac{x_{42}}{2u_h}\right)}} \left[x_{21} \coth\left(\frac{x_{21}}{2u_h}\right) + x_{43} \coth\left(\frac{x_{43}}{2u_h}\right) - x_{32} \coth\left(\frac{x_{32}}{2u_h}\right) - x_{41} \coth\left(\frac{x_{41}}{2u_h}\right) \right] \\
 & - \frac{u_c^2}{32G_N u_h^2} \left(\sqrt{\frac{\sinh\left(\frac{x_{31}}{2u_h}\right) \sinh\left(\frac{x_{42}}{2u_h}\right)}{\sinh\left(\frac{x_{21}}{2u_h}\right) \sinh\left(\frac{x_{43}}{2u_h}\right)}} \left[\operatorname{csch}^2\left(\frac{x_{31}}{2u_h}\right) + \operatorname{csch}^2\left(\frac{x_{42}}{2u_h}\right) - \operatorname{csch}^2\left(\frac{x_{32}}{2u_h}\right) - \operatorname{csch}^2\left(\frac{x_{41}}{2u_h}\right) \right] \right. \\
 & \left. + \sqrt{\frac{\sinh\left(\frac{x_{21}}{2u_h}\right) \sinh\left(\frac{x_{43}}{2u_h}\right)}{\sinh\left(\frac{x_{31}}{2u_h}\right) \sinh\left(\frac{x_{42}}{2u_h}\right)}} \left[\operatorname{csch}^2\left(\frac{x_{21}}{2u_h}\right) + \operatorname{csch}^2\left(\frac{x_{43}}{2u_h}\right) - \operatorname{csch}^2\left(\frac{x_{32}}{2u_h}\right) - \operatorname{csch}^2\left(\frac{x_{41}}{2u_h}\right) \right] \right). \quad (4.33)
 \end{aligned}$$

The first term in Eq. (4.33) is the EWCS between the two disjoint intervals for the corresponding undeformed CFT_2 . The rest of the terms (proportional to u_c^2 and thus to μ) describes the leading-order corrections to the EWCS due to the $\text{T}\bar{\text{T}}$ deformation. The third term becomes negligible (compared to the second term) in the high-temperature limit. The change in HEE for two disjoint intervals in proximity due to the $\text{T}\bar{\text{T}}$ deformation is given by [34]

$$\begin{aligned}
 \delta S(A \cup B) \\
 = -\frac{\mu c^2 \pi^4}{9\beta^3} \left[x_{32} \coth\left(\frac{\pi x_{32}}{\beta}\right) + x_{41} \coth\left(\frac{\pi x_{41}}{\beta}\right) \right]. \quad (4.34)
 \end{aligned}$$

The change in holographic OEE for two disjoint intervals due to the $\text{T}\bar{\text{T}}$ deformation may now be computed by combining Eqs. (4.33) and (4.34) through Eq. (2.14). Interestingly our holographic result matches exactly with our earlier field theory computation in Eq. (4.11), in the large central-charge limit together with small deformation parameter and high-temperature limits, which serves as a strong consistency check for our holographic construction.

2. Two adjacent intervals

We now consider two adjacent intervals $A = [x_1, x_2]$ and $B = [x_2, x_3]$ with $x_1 < x_2 < x_3$ as described in Sec. 4.1.2. The configuration has been depicted in Fig. 2. The EWCS

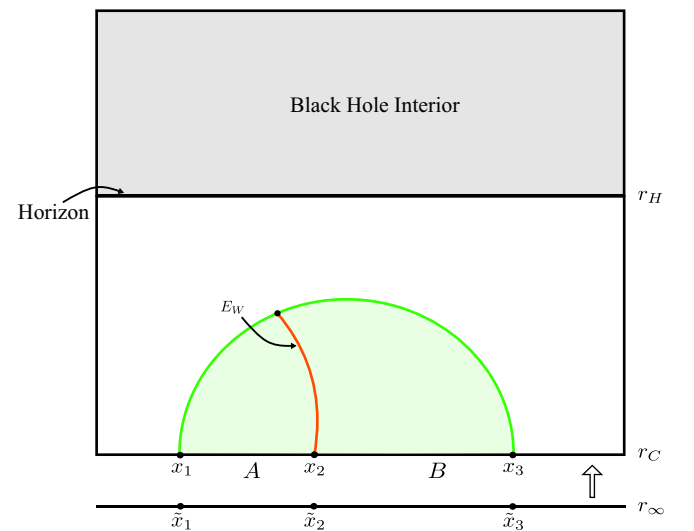


FIG. 2. EWCS for two adjacent intervals in a $\text{T}\bar{\text{T}}$ deformed CFT_2 . Figure based on [42].

for the corresponding bulk points $X(s_1), X(s_2), X(s_3)$ is given by [10]

$$E_W = \frac{1}{4G_N} \cosh^{-1} \left(\frac{\sqrt{2}}{\sqrt{v}} \right), \quad (4.35)$$

where

$$E_W(A:B) = \frac{1}{4G_N} \log \left[\frac{4u_h \sinh\left(\frac{x_{21}}{2u_h}\right) \sinh\left(\frac{x_{32}}{2u_h}\right)}{u_c \sinh\left(\frac{x_{31}}{2u_h}\right)} \right] - \frac{u_c^2}{16G_N u_h^3} \left[x_{21} \coth\left(\frac{x_{21}}{2u_h}\right) - x_{31} \coth\left(\frac{x_{31}}{2u_h}\right) + x_{32} \coth\left(\frac{x_{32}}{2u_h}\right) \right] + \frac{u_c^2}{16G_N u_h^2} \left[\operatorname{csch}^2\left(\frac{x_{21}}{2u_h}\right) - \operatorname{csch}^2\left(\frac{x_{31}}{2u_h}\right) + \operatorname{csch}^2\left(\frac{x_{32}}{2u_h}\right) \right]. \quad (4.37)$$

Similar to the disjoint configuration, the first term in Eq. (4.37) is the EWCS between the two adjacent intervals for the corresponding undeformed CFT_2 . The rest of the terms (proportional to u_c^2 and thus to μ) describe the leading-order corrections for the EWCS due to the $T\bar{T}$ deformation. The third term becomes negligible (compared to the second term) in the high-temperature limit. The change in HEE for two adjacent intervals due to the $T\bar{T}$ deformation is given by [34]

$$\delta S(A \cup B) = - \left(\frac{\mu c^2 \pi^4}{9\beta^3} \right) x_{31} \coth\left(\frac{\pi x_{31}}{\beta}\right). \quad (4.38)$$

The change in holographic OEE for two adjacent intervals due to the $T\bar{T}$ deformation may now be obtained from Eqs. (2.14), (4.37), and (4.38), and is described by Eq. (4.17), where as earlier we have used the holographic dictionary. Once again we find exact agreement between our holographic and field theory results (in the large central-charge limit, along with small deformation parameter and high-temperature limits), which substantiates our holographic construction.

Note that a limiting analysis of the EWCS for two disjoint intervals for the undeformed CFT_2 does not lead to the corresponding adjacent result given by the first term in Eq. (4.37). This mismatch is not surprising since for the case of disjoint intervals the EWCS is given by a minimal curve between two bulk geodesics whereas for adjacent intervals it is a minimal curve between a bulk geodesic and a boundary point. In this connection, we should not expect the corrections due to the $T\bar{T}$ deformations to have a well-defined adjacent limit as well.

3. A single interval

Finally we consider the case of a single interval $A = [-\ell, 0]$ in a thermal $T\bar{T}$ deformed holographic CFT_2

$$v = \frac{\xi_{13}^{-1}}{\xi_{12}^{-1} \xi_{23}^{-1}}, \quad \xi_{ij}^{-1} = -X(s_i) \cdot X(s_j). \quad (4.36)$$

As earlier the three points on the boundary may be expressed in the global coordinates as $X(0, r_c, x_i)$ for $i = 1, 2, 3$. The corresponding EWCS may then be computed from Eq. (4.35) as

($\ell > 0$). As described in Sec. IV A 3 this necessitates the introduction of two large but finite auxiliary intervals $B_1 = [-L, -\ell]$ and $B_2 = [0, L]$ sandwiching the interval A with $B \equiv B_1 \cup B_2$ ($L \gg \ell$) [48]. The situation has been outlined in Fig. 3.

We then compute the holographic OEE for this modified configuration, and finally take the bipartite limit $B \rightarrow A^c$ (implemented through $L \rightarrow \infty$) to obtain the desired OEE for the original configuration of the single interval A . The EWCS between the intervals A and $B = B_1 \cup B_2$ may be computed from the following relation [62–64]

$$\tilde{E}_W(A:B) = E_W(A:B_1) + E_W(A:B_2), \quad (4.39)$$

where $\tilde{E}_W(A:B)$ denotes an upper bound on the EWCS between the intervals A and B . All subsequent

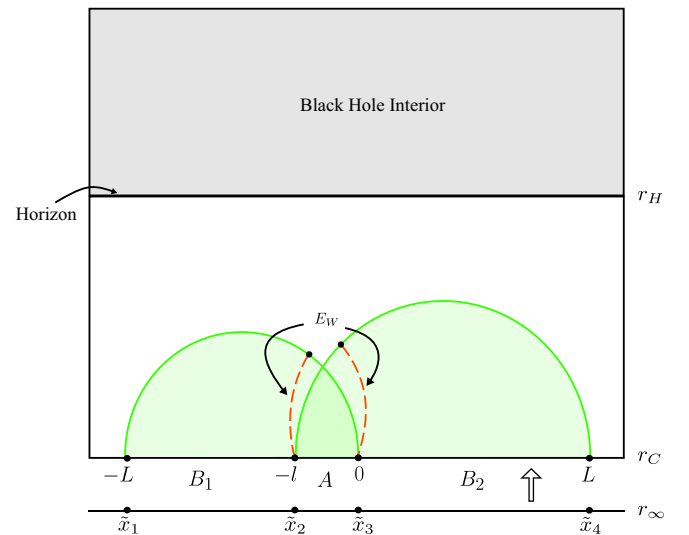


FIG. 3. EWCS for a single interval in a $T\bar{T}$ deformed CFT_2 . Figure based on [42].

computations involving Eq. (4.39) should be interpreted accordingly. Note that each term on the right-hand side of Eq. (4.39) represents the EWCS of two adjacent intervals which has already been computed in Sec. IV B 2. The corrections to these terms may thus be read off from Eq. (4.37) as follows:

$$\begin{aligned} \delta E_W(A: B_1) = & -\frac{u_c^2}{16G_N u_h^3} \left[\ell \coth\left(\frac{\ell}{2u_h}\right) \right. \\ & + (L - \ell) \coth\left(\frac{L - \ell}{2u_h}\right) \\ & \left. - L \coth\left(\frac{L}{2u_h}\right) \right], \end{aligned} \quad (4.40)$$

and

$$\begin{aligned} \delta E_W(A: B_2) = & -\frac{u_c^2}{16G_N u_h^3} \left[\ell \coth\left(\frac{\ell}{2u_h}\right) + L \coth\left(\frac{L}{2u_h}\right) \right. \\ & \left. - (L + \ell) \coth\left(\frac{L + \ell}{2u_h}\right) \right], \end{aligned} \quad (4.41)$$

where we have already taken the limits of small deformation parameter and high temperature. The correction to the HEE for a single interval is given as follows [34]:

$$\delta S(A \cup A^c) = -\left(\frac{2\mu c^2 \pi^4 L}{9\beta^3}\right) \coth\left(\frac{2\pi L}{\beta}\right), \quad (4.42)$$

where the bipartite limit has already been implemented. The correction to holographic OEE for a single interval due to the $\text{T}\bar{\text{T}}$ deformation may then be computed from Eqs. (4.39)–(4.42) through Eq. (2.14) on effecting the bipartite limit $L \rightarrow \infty$ as follows:

$$\begin{aligned} \delta S_o(A: A^c) = & -\frac{\mu c^2 \pi^4 \ell}{9\beta^3} \left[\coth\left(\frac{\pi \ell}{\beta}\right) - 1 \right] \\ & - \lim_{L \rightarrow \infty} \left[\frac{\mu c^2 \pi^4 L}{9\beta^3} \coth\left(\frac{2\pi L}{\beta}\right) \right], \end{aligned} \quad (4.43)$$

where we have utilized the holographic dictionary as earlier. Note that on taking the high-temperature limit ($\beta \rightarrow 0$), Eq. (4.22) reduces (the second part of the first term becomes negligible as $e^{-\frac{2\pi\ell}{\beta}} \rightarrow 0$) exactly to Eq. (4.43). This once again serves as a robust consistency check for our holographic construction.

We may understand the corrections to the thermal entropy described in Eq. (4.24) from a holographic viewpoint as well. Recall that the holographic entanglement entropy receives the thermal contribution as the corresponding RT surface wraps the black hole horizon [3]. Under the $\text{T}\bar{\text{T}}$ deformation, the holographic screen is pushed inside the bulk and the wrapping of the corresponding minimal surface around the black hole horizon is now smaller compared to the undeformed case. As a result, the contribution to the thermal entropy decreases compared to the undeformed case.

V. $\text{T}\bar{\text{T}}$ DEFORMED FINITE SIZE CFT_2 AND HOLOGRAPHY

A. OEE in a $\text{T}\bar{\text{T}}$ deformed finite size CFT_2

In this section we follow a similar prescription as in Sec. IV A to formulate a perturbative expansion for the OEE in a $\text{T}\bar{\text{T}}$ deformed finite-size CFT_2 of length L at zero temperature. For this setup, the corresponding manifold \mathcal{M} describes an infinitely long cylinder of circumference L with the length direction periodically compactified by the relation $x \sim x + L$ [47]. The cylindrical manifold \mathcal{M} for this configuration may be represented by the complex coordinates described in Eq. (4.1) with the spatial coordinate $x \in (0, L)$ and the time coordinate $\tau \in (-\infty, \infty)$ [47]. The cylinder \mathcal{M} may be further described on the complex plane \mathbb{C} through the following conformal map [47]

$$z = e^{-\frac{2\pi i w}{L}}, \quad \bar{z} = e^{\frac{2\pi i v}{L}}, \quad (5.1)$$

where (z, \bar{z}) are the coordinates on the complex plane. The relations in Eqs. (4.3) and (4.4) remain valid with β effectively replaced by iL . With these modifications, the expressions in Eqs. (3.1)–(3.3), and (3.5) may now be applied to compute the OEE in a $\text{T}\bar{\text{T}}$ deformed finite size CFT_2 at zero temperature.

1. Two disjoint intervals

As earlier we start with the mixed state of two disjoint spatial intervals $A = [x_1, x_2]$ and $B = [x_3, x_4]$ in a $\text{T}\bar{\text{T}}$ deformed finite size CFT_2 of length L at zero temperature, defined on the cylindrical manifold \mathcal{M} described above ($x_1 < x_2 < x_3 < x_4$). The first-order correction in the OEE of two disjoint intervals in a $\text{T}\bar{\text{T}}$ deformed finite size CFT_2 may be obtained by substituting Eqs. (4.5)–(4.8) along with Eq. (5.1) (β replaced by iL) into Eq. (3.5) as follows:

$$\begin{aligned}
 \delta S_o(A:B) &= \frac{-\mu c^2 \pi^4}{18L^4 (z_1 - z_3)^2 (z_2 - z_4)^2 (\eta - 1) \sqrt{\eta}} \\
 &\times \int_{\mathcal{M}} z^2 \left[\frac{(z_2 - z_3)(z_2 - z_4)((z - z_1)(z_3 - z_4) + (z_1 - z_3)(2z - 3z_1 + z_4)\sqrt{\eta})}{(z - z_1)^2} \right. \\
 &+ \frac{(z_1 - z_3)(z_1 - z_4)(-(z - z_2)(z_3 - z_4)) + (2z - 3z_2 + z_3)(z_2 - z_4)\sqrt{\eta}}{(z - z_2)^2} \\
 &- \frac{(z_1 - z_4)(z_2 - z_4)((z_1 - z_2)(-z + z_3) + (2z + z_2 - 3z_3)(z_1 - z_3)\sqrt{\eta})}{(z - z_3)^2} \\
 &\left. + \frac{(z_1 - z_3)(z_3 - z_2)((z_1 - z_2)(z - z_4) + (2z + z_1 - 3z_4)(z_2 - z_4)\sqrt{\eta})}{(z - z_4)^2} \right]. \quad (5.2)
 \end{aligned}$$

We now substitute $z \rightarrow e^{-\frac{2\pi i(x+i\tau)}{L}}$ into eq. (5.2) and integrate the resulting expression with respect to x to arrive at

$$\begin{aligned}
 \delta S_o(A:B) &= \frac{i\mu c^2 \pi^3}{36L^3 \sqrt{\eta}} \int d\tau \left[\frac{z_1 \sqrt{\eta}}{e^{\frac{2\pi(-ix+\tau)}{L}} - z_1} + \frac{z_2 \sqrt{\eta}}{e^{\frac{2\pi(-ix+\tau)}{L}} - z_2} + \frac{z_3 \sqrt{\eta}}{e^{\frac{2\pi(-ix+\tau)}{L}} - z_3} + \frac{z_4 \sqrt{\eta}}{e^{\frac{2\pi(-ix+\tau)}{L}} - z_4} \right. \\
 &+ \frac{(z_1(z_3 - z_4) + (z_1 - z_3)(z_1 + z_4)\sqrt{\eta}) \log[e^{\frac{2\pi(-ix+\tau)}{L}} - z_1]}{(z_1 - z_3)(z_1 - z_4)} \\
 &+ \frac{(z_2(z_4 - z_3) + (z_2 + z_3)(z_2 - z_4)\sqrt{\eta}) \log[e^{\frac{2\pi(-ix+\tau)}{L}} - z_2]}{(z_2 - z_3)(z_2 - z_4)} \\
 &+ \frac{((z_2 - z_1)z_3 + (z_1 - z_3)(z_2 + z_3)\sqrt{\eta}) \log[e^{\frac{2\pi(-ix+\tau)}{L}} - z_3]}{(z_1 - z_3)(z_3 - z_2)} \\
 &\left. + \frac{((z_2 - z_1)z_4 + (z_1 + z_4)(z_4 - z_2)\sqrt{\eta}) \log[e^{\frac{2\pi(-ix+\tau)}{L}} - z_4]}{(z_1 - z_4)(z_4 - z_2)} \right]. \quad (5.3)
 \end{aligned}$$

We observe that the first four terms on the right hand side of Eq. (5.3) readily vanish on inserting the limits of integration $x = 0$ and $x = L$. Since we have considered the system on a constant time slice, we may take τ_j ($j = 1, 2, 3, 4$) to be zero for all boundary points, and the contributions of the logarithmic functions become zero identically. Thus it is observed that the resultant integrand for the τ integration in Eq. (5.3) vanishes leading to no nontrivial first-order correction to the OEE. This is in conformity with the vanishing entanglement entropy for a finite sized $\overline{\text{T}\overline{\text{T}}}$ deformed CFT_2 [32].

2. Two adjacent intervals

We now focus on the bipartite mixed state of two adjacent intervals $A = [x_1, x_2]$ and $B = [x_2, x_3]$ in a $\overline{\text{T}\overline{\text{T}}}$ deformed finite size CFT_2 of length L at zero temperature, defined on the cylindrical manifold \mathcal{M} described by Eqs. (4.1) and (5.1) ($x_1 < x_2 < x_3$). For this case, Eqs. (3.5), (4.12), (4.13), and (4.14) may still be employed along with the relation described in Eq. (5.1), effectively replacing β by iL . The first-order correction in OEE due to μ for two adjacent intervals is then given by

$$\begin{aligned}
 \delta S_o(A:B) &= -\frac{\mu c^2 \pi^4}{18L^4} \int_{\mathcal{M}} \frac{z^2}{(z - z_1)^2 (z - z_2)^2 (z - z_3)^2} \\
 &\times \left[z_2^2 z_3^2 - z_1 z_2 z_3 (z_2 + z_3) + z_1^2 (z_2^2 - z_2 z_3 + z_3^2) \right. \\
 &+ z^2 (z_1^2 + z_2^2 - z_2 z_3 + z_3^2 - z_1 (z_2 + z_3)) \\
 &- z (z_1^2 (z_2 + z_3) + z_2 z_3 (z_2 + z_3)) \\
 &\left. + z_1 (z_2^2 - 6z_2 z_3 + z_3^2) \right]. \quad (5.4)
 \end{aligned}$$

Next we replace $z \rightarrow e^{-\frac{2\pi i(x+i\tau)}{L}}$ into Eq. (5.4) and subsequently integrate with respect to x to obtain

$$\begin{aligned}
 \delta S_o(A:B) &= \frac{i\mu c^2 \pi^3}{36L^3} \int d\tau \left[\frac{z_1}{e^{\frac{2\pi(-ix+\tau)}{L}} - z_1} + \frac{z_2}{e^{\frac{2\pi(-ix+\tau)}{L}} - z_2} \right. \\
 &+ \frac{z_3}{e^{\frac{2\pi(-ix+\tau)}{L}} - z_3} + \frac{(z_1^2 - z_2 z_3) \log[e^{\frac{2\pi(-ix+\tau)}{L}} - z_1]}{(z_1 - z_2)(z_1 - z_3)} \\
 &+ \frac{(z_2^2 - z_1 z_3) \log[e^{\frac{2\pi(-ix+\tau)}{L}} - z_2]}{(z_2 - z_1)(z_2 - z_3)} \\
 &\left. + \frac{(z_3^2 - z_2 z_1) \log[e^{\frac{2\pi(-ix+\tau)}{L}} - z_3]}{(z_1 - z_3)(z_2 - z_3)} \right]. \quad (5.5)
 \end{aligned}$$

Similar to the disjoint case, the first three terms on the right hand side of Eq. (5.5) readily vanish when the limits of integration $x = 0$ and $x = L$ are inserted. As earlier, for a constant time slice $\tau_j = 0$ ($j = 1, 2, 3$), the logarithmic functions also contribute nothing to the definite integral. The resulting integrand for the τ integration in Eq. (5.5) thus vanishes. Hence, the corresponding first-order correction in the OEE of two adjacent intervals turns out to be zero.

3. A single interval

Finally we turn our attention to the bipartite mixed state configuration of a single interval $A = [x_1, x_2]$ in a $\text{T}\bar{\text{T}}$

$$\int_{\mathcal{M}_{n_o}} \langle T\bar{T} \rangle_{\mathcal{M}_{n_o}} = \frac{1}{n_o} \int_{\mathcal{M}} \frac{1}{\langle \sigma_{n_o}^2(z_1, \bar{z}_1) \bar{\sigma}_{n_o}^2(z_2, \bar{z}_2) \rangle} \left[\frac{\pi^2 c n_o}{6L^2} - \left(\frac{2\pi z}{L} \right)^2 \sum_{j=1}^2 \left(\frac{h_j}{(z - z_j)^2} + \frac{1}{(z - z_j)} \partial_{z_j} \right) \right] \times \left[\frac{\pi^2 c n_o}{6L^2} - \left(\frac{2\pi \bar{z}}{L} \right)^2 \sum_{k=1}^2 \left(\frac{\bar{h}_k}{(\bar{z} - \bar{z}_k)^2} + \frac{1}{(\bar{z} - \bar{z}_k)} \partial_{\bar{z}_k} \right) \right] \langle \sigma_{n_o}^2(z_1, \bar{z}_1) \bar{\sigma}_{n_o}^2(z_2, \bar{z}_2) \rangle_C, \quad (5.6)$$

where $h_1 = h_2 = h_{n_o}^{(2)}$ with $\bar{h}_i = h_i$ ($i = 1, 2$) [see Eqs. (2.11) and (2.12)]. The corresponding two-point twist correlator for this configuration is given by [47]

$$\langle \sigma_{n_o}^2(z_1, \bar{z}_1) \bar{\sigma}_{n_o}^2(z_2, \bar{z}_2) \rangle = \frac{\mathcal{C}_{12}}{|z_1 - z_2|^{2h_{n_o}}}, \quad (5.7)$$

where \mathcal{C}_{12} is the relevant normalization constant. Following a similar procedure like the earlier cases, the first-order

deformed finite size CFT_2 of length L at zero temperature, defined on the cylindrical manifold \mathcal{M} given in Eqs. (4.1) and (5.1) ($x_1 < x_2$). The construction of the relevant partially transposed reduced density matrix for this configuration is described in [47]. Once again we may utilize Eqs. (4.18) and (4.19) with only two points z_1 and z_2 , subject to Eq. (5.1) (with the effect of iL replacing β), and a two-point twist correlator as mentioned below in Eq. (5.7). We have expressed the modified version of Eq. (4.19) as applicable for the system under consideration for convenience of the reader as follows:

correction for the OEE of this setup may be given as follows:

$$\delta S_o(A:B) = -\frac{\mu c^2 \pi^4}{18L^4} (z_1 - z_2)^2 \int_{\mathcal{M}} \frac{z^2}{(z - z_1)^2 (z - z_2)^2}. \quad (5.8)$$

We then obtain the following expression by substituting $z \rightarrow e^{-\frac{2\pi i(x+i\tau)}{L}}$ into Eq. (5.8) and integrating with respect to x

$$\delta S_o(A:B) = \frac{i\mu c^2 \pi^3}{36L^3} \int d\tau \left[\frac{z_1}{e^{\frac{2\pi(-ix+\tau)}{L}} - z_1} + \frac{z_2}{e^{\frac{2\pi(-ix+\tau)}{L}} - z_2} + \frac{z_1 + z_2}{z_1 - z_2} \left(\log \left[e^{\frac{2\pi(-ix+\tau)}{L}} - z_1 \right] - \log \left[e^{\frac{2\pi(-ix+\tau)}{L}} - z_2 \right] \right) \right]. \quad (5.9)$$

Like the previous cases, we observe that the first two terms in eq. (5.9) vanish on implementation of the limits of integration $x = 0$ and $x = L$. As the system under consideration is on a constant time slice $\tau_j = 0$ ($j = 1, 2$), once again the terms containing the logarithmic functions also vanish. Again the resulting integrand for the τ integration in eq. (5.9) vanishes, indicating the vanishing of the first-order corrections of the OEE as earlier.

B. Holographic OEE in a $\text{T}\bar{\text{T}}$ deformed finite size CFT_2

The bulk dual of a $\text{T}\bar{\text{T}}$ deformed finite size CFT_2 of length L at zero temperature is represented by a finite cutoff AdS_3 geometry expressed in global coordinates as follows [1,2]:

$$ds^2 = R^2(-\cosh^2 \rho d\tau^2 + \sinh^2 \rho d\phi^2 + d\rho^2), \quad (5.10)$$

where $\phi = 2\pi x/L$. As earlier we embed this AdS_3 geometry in $\mathbb{R}^{2,2}$ as follows [10]:

$$ds^2 = \eta_{AB} dX^A dX^B = -dX_0^2 - dX_1^2 + dX_2^2 + dX_3^2, \quad X^2 = -1. \quad (5.11)$$

The metric in Eq. (5.10) may be expressed in terms of the embedding coordinates introduced in Eq. (5.11) as follows:

$$\begin{aligned} X_0(\tau, \phi, \rho) &= R \cosh \rho \sin \tau, \\ X_1(\tau, \phi, \rho) &= R \cosh \rho \cos \tau, \\ X_2(\tau, \phi, \rho) &= R \sinh \rho \cos \phi, \\ X_3(\tau, \phi, \rho) &= R \sinh \rho \sin \phi. \end{aligned} \quad (5.12)$$

The finite cutoff of the AdS_3 geometry is located at $\rho = \rho_c$, where

$$\cosh \rho_c = \sqrt{\frac{3L^2}{2\mu\epsilon\pi^3}}. \quad (5.13)$$

With the UV cutoff of the field theory given by $\epsilon = \sqrt{\mu\epsilon\pi/6}$ [see Eq. (4.25)], the relation in Eq. (5.13) may be rewritten as

$$\cosh \rho_c = \frac{L}{2\pi\epsilon}. \quad (5.14)$$

1. Two disjoint intervals

We begin with two disjoint spatial intervals $A = [x_1, x_2]$ and $B = [x_3, x_4]$ on a cylindrical manifold \mathcal{M} as detailed in Sec. VA 1 ($x_1 < x_2 < x_3 < x_4$). Note that the EWCS

involving arbitrary bulk points $X(s_1), X(s_2), X(s_3), X(s_4)$ for a $\overline{\text{T}\overline{\text{T}}}$ deformed finite size CFT_2 is described by [10]

$$E_W = \frac{1}{4G_N} \cosh^{-1} \left(\frac{1 + \sqrt{u}}{\sqrt{v}} \right), \quad (5.15)$$

where

$$u = \frac{\xi_{12}^{-1} \xi_{34}^{-1}}{\xi_{13}^{-1} \xi_{24}^{-1}}, \quad v = \frac{\xi_{14}^{-1} \xi_{23}^{-1}}{\xi_{13}^{-1} \xi_{24}^{-1}}, \quad \xi_{ij}^{-1} = -X(s_i) \cdot X(s_j). \quad (5.16)$$

The end points of the two disjoint intervals under consideration on the boundary may be represented by the embedding coordinates as $X(0, \phi_i, \rho_c)$ for $i = 1, 2, 3, 4$, where $\phi_1 < \phi_2 < \phi_3 < \phi_4$ (Note that $\phi_i = 2\pi x_i/L$). The corresponding EWCS may then be computed from Eq. (5.15) as

$$E_W(A:B) = \frac{1}{4G_N} \cosh^{-1} \left(\sqrt{\frac{[1 + \sin^2(\frac{\pi x_{31}}{L}) \sinh^2 \rho_c][1 + \sin^2(\frac{\pi x_{42}}{L}) \sinh^2 \rho_c]}{[1 + \sin^2(\frac{\pi x_{32}}{L}) \sinh^2 \rho_c][1 + \sin^2(\frac{\pi x_{41}}{L}) \sinh^2 \rho_c]}} \right) + \sqrt{\frac{[1 + \sin^2(\frac{\pi x_{21}}{L}) \sinh^2 \rho_c][1 + \sin^2(\frac{\pi x_{43}}{L}) \sinh^2 \rho_c]}{[1 + \sin^2(\frac{\pi x_{32}}{L}) \sinh^2 \rho_c][1 + \sin^2(\frac{\pi x_{41}}{L}) \sinh^2 \rho_c]}}. \quad (5.17)$$

To extract the desired first-order corrections, we now expand Eq. (5.17) in small $(1/\cosh \rho_c)$ as follows:

$$E_W(A:B) = \frac{1}{4G_N} \cosh^{-1} \left[1 + 2 \frac{\sin(\frac{\pi x_{21}}{L}) \sin(\frac{\pi x_{43}}{L})}{\sin(\frac{\pi x_{32}}{L}) \sin(\frac{\pi x_{41}}{L})} \right] + \mathcal{O}[\epsilon^2], \quad (5.18)$$

where we have utilized Eq. (5.14) to substitute ϵ . The first term in Eq. (5.18) is the EWCS between the two disjoint intervals for the corresponding undeformed CFT_2 . The rest of the terms characterizing the corrections for the EWCS due to the $\overline{\text{T}\overline{\text{T}}}$ deformation are second order and higher in ϵ and thus negligible. The corresponding leading-order corrections for the HEE due to the $\overline{\text{T}\overline{\text{T}}}$ deformation has been shown to be zero [32]. Thus the leading-order corrections to the holographic OEE of two disjoint intervals in a $\overline{\text{T}\overline{\text{T}}}$ deformed finite size CFT_2 is zero, which is in complete agreement with our corresponding field theory computations in the large central charge limit described in Sec. VA 1.

The vanishing of the EWCS as well as the entanglement entropy may be attributed to the fact that in $\overline{\text{T}\overline{\text{T}}}$ deformed finite sized CFT_2 s, the lengths of the intervals do not

depend on the cutoff radius in Eq. (5.13). In contrast, for thermal CFT_2 s the lengths of the intervals depend non-trivially [cf. Eq. (4.27)] on the cutoff radius r_c as long as $r_h \neq 0$ (or, $1/\beta \neq 0$) [32]. We will discuss this issue further in Sec. VI.

2. Two adjacent intervals

We now turn our attention to the case of two adjacent intervals $A = [x_1, x_2]$ and $B = [x_2, x_3]$ ($x_1 < x_2 < x_3$) as described in Sec. VA 2. The bulk description of the end points of the intervals A and B for a $\overline{\text{T}\overline{\text{T}}}$ deformed finite-size CFT_2 is given by $X(0, \phi_i, \rho_c)$ for $i = 1, 2, 3$, where $\phi_1 < \phi_2 < \phi_3$ ($\phi_i = 2\pi x_i/L$). The EWCS for this configuration is described as follows [10]:

$$E_W = \frac{1}{4G_N} \cosh^{-1} \left(\frac{\sqrt{2}}{\sqrt{v}} \right), \quad (5.19)$$

where

$$v = \frac{\xi_{13}^{-1}}{\xi_{12}^{-1} \xi_{23}^{-1}}, \quad \xi_{ij}^{-1} = -X(s_i) \cdot X(s_j). \quad (5.20)$$

We now utilize Eq. (5.19) to explicitly compute the EWCS as follows:

$$E_W(A:B) = \frac{1}{4G_N} \cosh^{-1} \left(\sqrt{\frac{2[\cosh^2(\rho_c) - \cos(\frac{2\pi x_{21}}{L})\sinh^2(\rho_c)][\cosh^2(\rho_c) - \cos(\frac{2\pi x_{32}}{L})\sinh^2(\rho_c)]}{\cosh^2(\rho_c) - \cos(\frac{2\pi x_{31}}{L})\sinh^2(\rho_c)}}} \right). \quad (5.21)$$

We are now in a position to extract the leading-order corrections to the EWCS from Eq. (5.21) by expanding in small $(1/\cosh\rho_c)$ as follows:

$$E_W(A:B) = \frac{1}{4G_N} \log \left[\left(\frac{2L}{\pi\epsilon} \right) \frac{\sin(\frac{\pi x_{21}}{L}) \sin(\frac{\pi x_{32}}{L})}{\sin(\frac{\pi x_{31}}{L})} \right] + \mathcal{O}[\epsilon^2], \quad (5.22)$$

where we have already substituted the relation in Eq. (5.14). As earlier the first term on the right-hand side of Eq. (5.22) describes the EWCS between the two adjacent intervals for the corresponding undeformed CFT_2 . Again the $\text{T}\bar{\text{T}}$ correction terms are second order and higher in ϵ and negligible. The leading-order corrections of the HEE for this configuration due to the $\text{T}\bar{\text{T}}$ deformation has been demonstrated to be vanishing [32]. Hence, the leading-order corrections to the holographic OEE for this case vanishes, which once again is in conformity with our field theory results in the large central-charge limit described in Sec. VA 2.

3. A single interval

The bulk representation of the end points of a single interval of length ℓ may be given by $X(0, 0, \rho_c)$ and $X(0, \delta\phi, \rho_c)$, where $\delta\phi = \frac{2\pi\ell}{L}$. The EWCS for the given configuration (same as the HEE for a single interval) may be computed as

$$E_W(A:A^c) = \frac{1}{4G_N} \cosh^{-1} \left[1 + 2\sinh^2(\rho_c) \sin^2\left(\frac{\pi\ell}{L}\right) \right]. \quad (5.23)$$

Once again Eq. (5.23) may be expanded for small $(1/\cosh\rho_c)$ to obtain the following expression for the EWCS:

$$E_W(A:A^c) = \frac{1}{2G_N} \log \left[\frac{L}{\pi\epsilon} \sin\left(\frac{\pi\ell}{L}\right) \right] + \mathcal{O}[\epsilon^2], \quad (5.24)$$

where we have used Eq. (5.14) to replace $\cosh\rho_c$. Once again the first term of Eq. (5.24) represents the EWCS of a single interval for the corresponding undeformed CFT_2 , while we have neglected the second- and higher-order correction terms in ϵ . The corresponding corrections for the HEE of a single interval has been shown to be zero [32].

Thus the leading-order corrections to the holographic OEE for a single interval vanishes, demonstrating agreement with our field theory calculations in the large central charge limit detailed in Sec. VA 3.

VI. SUMMARY AND DISCUSSIONS

To summarize we have computed the OEE for different bipartite mixed-state configurations in a $\text{T}\bar{\text{T}}$ deformed finite-temperature CFT_2 with a small deformation parameter μ . In this context we have developed a perturbative construction to compute the first-order correction to the OEE for small deformation parameter through a suitable replica technique. This incorporates definite integrals of the expectation value of the $\text{T}\bar{\text{T}}$ operator over an n_o sheeted replica manifold. We have been able to express these expectation values in terms of appropriate twist-field correlators for the configurations under consideration. Utilizing our perturbative construction we have subsequently computed the OEE for the mixed-state configurations described by two disjoint intervals, two adjacent intervals, and a single interval in a $\text{T}\bar{\text{T}}$ deformed thermal CFT_2 .

Following the above we have computed the corresponding EWCS in the dual bulk finite cutoff BTZ black hole geometry for the above configurations utilizing an embedding coordinate technique in the literature. Interestingly it was possible to demonstrate that the first-order correction to the sum of the EWCS and the corresponding HEE matched exactly with the first-order correction to the CFT_2 replica technique results for the OEE in the large central-charge and high-temperature limit. This extends the holographic duality for the OEE proposed in the literature to $\text{T}\bar{\text{T}}$ deformed thermal CFT_2 s.

Finally we have extended our perturbative construction to $\text{T}\bar{\text{T}}$ deformed finite size CFT_2 s at zero temperature. We have computed the first-order corrections to the OEE for the configurations mentioned earlier in such CFT_2 s in the large central-charge limit. In all the cases we have been able to show that the leading-order corrections vanish in the appropriate limits. Quite interestingly it was possible to demonstrate that the first-order corrections to the corresponding bulk EWCS in the dual cutoff BTZ geometry were also identically zero in a further validation of the extension of the holographic duality for the OEE in the literature to $\text{T}\bar{\text{T}}$ deformed finite size CFT_2 s at zero temperature.

There are several recurring features of our results. Note that when the intervals are located along a compactified

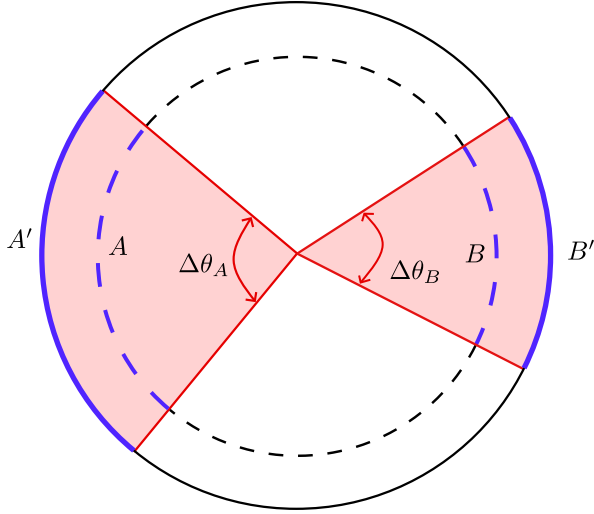


FIG. 4. Schematics of two disjoint intervals placed along the compactified direction in a holographic $\bar{\text{T}}\bar{\text{T}}$ deformed CFT_2 . The undashed (dashed) circle denotes the location of the holographic screens before (after) the $\bar{\text{T}}\bar{\text{T}}$ deformation.

direction, there are no $\bar{\text{T}}\bar{\text{T}}$ corrections as the angular separations of the subsystems are not affected by pushing the holographic screen inside the bulk [65], as depicted in Fig. 4. On the other hand, when this direction is non-compact, the spatial extents of the subsystems become dependent on the finite cutoff radius as depicted in Figs. 2, 1, and 3, and hence there will be appropriate $\bar{\text{T}}\bar{\text{T}}$ corrections [65]. For thermal CFT_2 s, the time direction is compactified, but the intervals are spatial and hence situated along the spatial direction. Thus for thermal CFT_2 s our results

indicated corrections due to the $\bar{\text{T}}\bar{\text{T}}$ deformations. For finite-size CFT_2 s, the space direction is compactified, and the corresponding corrections vanish.

It will be instructive to develop similar constructions for other entanglement measures such as entanglement of purification, balanced partial entanglement, reflected entropy etc. for $\bar{\text{T}}\bar{\text{T}}$ deformed CFT_2 s. Also a covariant framework for holographic entanglement in these theories along the lines of the HRT construction is an important open issue. Furthermore, it will be interesting to extend our analysis to $\bar{\text{T}}\bar{\text{T}}$ deformations of thermal CFT_2 with conserved charges. These constitute exciting open problems for the future.

ACKNOWLEDGMENTS

We would like to thank Lavish, Mir Afrasiar and Himanshu Chourasiya for valuable discussions. The work of G. S. is supported in part by the Dr. Jag Mohan Garg Chair Professor position at the Indian Institute of Technology, Kanpur. The work of S. B. is supported by the Council of Scientific and Industrial Research (CSIR) of India under Grant No. 09/0092(12686)/2021-EMR-I.

APPENDIX: THE INTEGRALS FOR THERMAL CFT_2 s

The detailed derivation of the integrals appearing in Eqs. (4.9), (4.15), and (4.21) has been provided in this appendix. Note that the corresponding domain of integration for all the configurations is the cylindrical manifold \mathcal{M} characterized by the complex coordinates (w, \bar{w}) [see Eqs. (4.1) and (4.2)].

1. Two disjoint intervals

The holomorphic part of the integral in Eq. (4.9) may be written as

$$\begin{aligned}
 & -\frac{\mu c^2 \pi^4 \sqrt{\eta}}{18\beta^4 z_{21} z_{32} z_{41} z_{43}} \int_{\mathcal{M}} d^2 w(z^2) \left[\frac{z_{32} z_{42} [z_{31} (2z - 3z_1 + z_4) \sqrt{\eta} + z_{43} (z - z_1)]}{(z - z_1)^2} + \frac{z_{31} z_{41} [z_{42} (2z - 3z_2 + z_3) \sqrt{\eta} - z_{43} (z - z_2)]}{(z - z_2)^2} \right. \\
 & \left. - \frac{z_{42} z_{41} [z_{31} (2z + z_2 - 3z_3) \sqrt{\eta} - z_{21} (z - z_3)]}{(z - z_3)^2} - \frac{z_{31} z_{32} [z_{42} (2z + z_1 - 3z_4) \sqrt{\eta} + z_{21} (z - z_4)]}{(z - z_4)^2} \right] \quad (\text{A1})
 \end{aligned}$$

$$\begin{aligned}
 & = -\frac{\mu c^2 \pi^4 \sqrt{\eta}}{18\beta^4 z_{21} z_{32} z_{41} z_{43}} \int_0^\infty dx \int_0^\beta dt e^{\frac{4\pi(x+it)}{\beta}} \left[\frac{z_{32} z_{42} [z_{31} (2e^{\frac{2\pi(x+it)}{\beta}} - 3z_1 + z_4) \sqrt{\eta} + z_{43} (e^{\frac{2\pi(x+it)}{\beta}} - z_1)]}{(e^{\frac{2\pi(x+it)}{\beta}} - z_1)^2} \right. \\
 & + \frac{z_{31} z_{41} [z_{42} (2e^{\frac{2\pi(x+it)}{\beta}} - 3z_2 + z_3) \sqrt{\eta} - z_{43} (e^{\frac{2\pi(x+it)}{\beta}} - z_2)]}{(e^{\frac{2\pi(x+it)}{\beta}} - z_2)^2} - \frac{z_{42} z_{41} [z_{31} (2e^{\frac{2\pi(x+it)}{\beta}} + z_2 - 3z_3) \sqrt{\eta} - z_{21} (e^{\frac{2\pi(x+it)}{\beta}} - z_3)]}{(e^{\frac{2\pi(x+it)}{\beta}} - z_3)^2} \\
 & \left. - \frac{z_{31} z_{32} [z_{42} (2e^{\frac{2\pi(x+it)}{\beta}} + z_1 - 3z_4) \sqrt{\eta} + z_{21} (e^{\frac{2\pi(x+it)}{\beta}} - z_4)]}{(e^{\frac{2\pi(x+it)}{\beta}} - z_4)^2} \right]. \quad (\text{A2})
 \end{aligned}$$

The primitive function on indefinite integration with respect to τ turns out to be

$$\begin{aligned}
& -\frac{i\mu c^2 \pi^3}{36\beta^3 \sqrt{\eta}} \left[\frac{(\sqrt{\eta}z_1^2 + (\sqrt{\eta}-1)z_1(z_{43}) - \sqrt{\eta}z_3z_4) \log(-z_1 + e^{\frac{2\pi(x+i\tau)}{\beta}})}{z_{31}z_{41}} \right. \\
& + \frac{(\sqrt{\eta}z_2^2 + (\sqrt{\eta}-1)z_2z_{34} - \sqrt{\eta}z_3z_4) \log(-z_2 + e^{\frac{2\pi(x+i\tau)}{\beta}})}{z_{32}z_{42}} \\
& - \frac{(\sqrt{\eta}z_1z_2 + (\sqrt{\eta}-1)z_1z_3 + z_3(-\sqrt{\eta}z_2 + z_2 - \sqrt{\eta}z_3)) \log(-z_3 + e^{\frac{2\pi(x+i\tau)}{\beta}})}{z_{31}z_{32}} \\
& \left. + \frac{(z_4(-\sqrt{\eta}z_2 + z_2 + \sqrt{\eta}z_4) - z_1(\sqrt{\eta}z_2 - \sqrt{\eta}z_4 + z_4)) \log(-z_4 + e^{\frac{2\pi(x+i\tau)}{\beta}})}{z_{41}z_{42}} \right]. \quad (\text{A3})
\end{aligned}$$

Due to the presence of branch points, the logarithmic functions necessitate careful treatment while implementing the limits of integration $\tau = 0$ and $\tau = \beta$. The following relation outlines the contribution due to a branch point at $z = z_j$ [32,34]

$$\log\left(e^{\frac{2\pi(x+i\tau)}{\beta}} - z_j\right)\Big|_{\tau=0}^{\tau=\beta} = \begin{cases} 2\pi i, & \text{for } e^{\frac{2\pi x}{\beta}} > z_j \Leftrightarrow x > \frac{\beta}{2\pi} \log z_j, \\ 0, & \text{otherwise.} \end{cases} \quad (\text{A4})$$

The branch cuts of the logarithmic functions change the limits of the x integrals as follows:

$$\int_{-\infty}^{\infty} dx \rightarrow \int_{\frac{\beta}{2\pi} \log z_j}^{\infty} dx, \quad \text{for } j = 1, 2, 3, 4.$$

We are now in a position to integrate over x and utilize the prescription described above to implement the limits of integration to arrive at

$$\frac{\mu c^2 \pi^3}{36\beta^2} \left(\frac{\left(z_1 \left(1 + \sqrt{\frac{z_{42}z_{43}}{z_{21}z_{31}} + z_4}\right)\right)}{z_{41}} \log\left[\frac{z_1}{z_2}\right] + \frac{\left(-2 + \sqrt{\frac{z_{21}z_{43}}{z_{31}z_{42}}}\right)(z_1z_2 - z_3z_4)}{z_{32}z_{41}} \log\left[\frac{z_2}{z_3}\right] + \frac{\left(z_1 + \left(1 + \sqrt{\frac{z_{12}z_{31}}{z_{42}z_{43}}}\right)z_4\right)}{z_{41}} \log\left[\frac{z_3}{z_4}\right] \right). \quad (\text{A5})$$

The anti holomorphic part of the integral in Eq. (4.9) follows a similar analysis and produces the same result as the holomorphic part.

2. Two adjacent intervals

The holomorphic part of the integral in Eq. (4.15) may be written as

$$\begin{aligned}
& \int_{\mathcal{M}} z^2 \left[\frac{1}{(z-z_1)^2} + \frac{1}{(z-z_2)^2} + \frac{1}{(z-z_3)^2} + \frac{(-3z + z_1 + z_2 + z_3)}{(z-z_1)(z-z_2)(z-z_3)} \right] \\
& = \int_{-\infty}^{\infty} dx \int_0^{\beta} d\tau e^{\frac{4\pi(x+i\tau)}{\beta}} \left[\frac{1}{\left(e^{\frac{2\pi(x+i\tau)}{\beta}} - z_1\right)^2} + \frac{1}{\left(e^{\frac{2\pi(x+i\tau)}{\beta}} - z_2\right)^2} + \frac{1}{\left(e^{\frac{2\pi(x+i\tau)}{\beta}} - z_3\right)^2} + \frac{z_1 + z_2 + z_3 - 3e^{\frac{2\pi(x+i\tau)}{\beta}}}{\left(e^{\frac{2\pi(x+i\tau)}{\beta}} - z_1\right)\left(e^{\frac{2\pi(x+i\tau)}{\beta}} - z_2\right)\left(e^{\frac{2\pi(x+i\tau)}{\beta}} - z_3\right)} \right]. \quad (\text{A6})
\end{aligned}$$

We proceed in a similar manner to the disjoint configuration as described in Appendix A 1. The indefinite integration with respect to τ leads to the following primitive function:

$$\begin{aligned}
& \frac{z_1}{e^{\frac{2\pi(x+i\tau)}{\beta}} - z_1} + \frac{z_2}{e^{\frac{2\pi(x+i\tau)}{\beta}} - z_2} + \frac{z_3}{e^{\frac{2\pi(x+i\tau)}{\beta}} - z_3} + \frac{(z_1^2 - z_2z_3)}{(z_1 - z_2)(z_1 - z_3)} \log\left(e^{\frac{2\pi(x+i\tau)}{\beta}} - z_1\right) \\
& + \frac{(z_1z_3 - z_2^2)}{(z_1 - z_2)(z_2 - z_3)} \log\left(e^{\frac{2\pi(x+i\tau)}{\beta}} - z_2\right) + \frac{(z_3^2 - z_1z_2)}{(z_1 - z_3)(z_2 - z_3)} \log\left(e^{\frac{2\pi(x+i\tau)}{\beta}} - z_3\right). \quad (\text{A7})
\end{aligned}$$

On implementation of the limits of integration $\tau = 0$ and $\tau = \beta$, the nonlogarithmic terms in the above expression vanish, while the contributions of the logarithmic terms follow the relation in Eq. (A4). Due to the relation in Eq. (A4), the limits of integration over x for each term in the integrand gets modified as follows:

$$\int_{-\infty}^{\infty} dx \rightarrow \int_{\frac{\beta}{2\pi} \log z_j}^{\infty} dx, \quad \text{for } j = 1, 2, 3.$$

The integration over x may now be performed to arrive at

$$\int_{\mathcal{M}} z^2 \left[\frac{1}{(z-z_1)^2} + \frac{1}{(z-z_2)^2} + \frac{1}{(z-z_3)^2} + \frac{(-3z+z_1+z_2+z_3)}{(z-z_1)(z-z_2)(z-z_3)} \right] = \frac{\beta^2}{2\pi} \left[\frac{(z_1^2 - z_2 z_3) \log(\frac{z_1}{z_2})}{z_{12} z_{13}} + \frac{(z_1 z_2 - z_3^2) \log(\frac{z_2}{z_3})}{z_{23} z_{13}} \right]. \quad (\text{A8})$$

As earlier, the antiholomorphic part of the integral gives result identical to the holomorphic part.

3. A single interval

The holomorphic part of the integral in Eq. (4.21) is given by

$$\begin{aligned} & \int_{\mathcal{M}} d^2 w \sum_{j=1}^4 \left(\frac{z^2}{(z-z_j)^2} - \frac{z^2}{(z-z_j)} \partial_{z_j} \log [z_{41}^2 z_{23}^2 \eta f(\eta)] \right) \\ &= \int_0^{\infty} dx \int_0^{\beta} d\tau e^{\frac{4\pi(x+i\tau)}{\beta}} \left[\sum_{j=1}^4 \frac{1}{(e^{\frac{2\pi(x+i\tau)}{\beta}} - z_j)^2} \right. \\ & \quad + \frac{-4e^{\frac{4\pi(x+i\tau)}{\beta}} - 2z_3 z_2 + z_1(-z_2 + z_3 - 2z_4) + z_2 z_4 - z_3 z_4 + 2e^{\frac{2\pi(x+i\tau)}{\beta}}(z_1 + z_2 + z_3 + z_4)}{(e^{\frac{2\pi(x+i\tau)}{\beta}} - z_1)(e^{\frac{2\pi(x+i\tau)}{\beta}} - z_2)(e^{\frac{2\pi(x+i\tau)}{\beta}} - z_3)(e^{\frac{2\pi(x+i\tau)}{\beta}} - z_4)} \\ & \quad \left. - \frac{z_{21} z_{32} z_{41} z_{43} f'(\eta)}{(e^{\frac{2\pi(x+i\tau)}{\beta}} - z_1)(e^{\frac{2\pi(x+i\tau)}{\beta}} - z_2)(e^{\frac{2\pi(x+i\tau)}{\beta}} - z_3)(e^{\frac{2\pi(x+i\tau)}{\beta}} - z_4) z_{31} z_{42} f(\eta)} \right]. \quad (\text{A9}) \end{aligned}$$

The indefinite integration over τ gives

$$\frac{i\beta}{2\pi} \sum_{j=1}^4 [B_j + C_j \log(e^{\frac{2\pi(x+i\tau)}{\beta}} - z_j)], \quad (\text{A10})$$

where

$$B_j = \frac{z_j}{e^{\frac{2\pi(x+i\tau)}{\beta}} - z_j}, \quad j = 1, 2, 3, 4, \quad (\text{A11})$$

and $C_1, C_2, C_3,$ and C_4 are given as follows:

$$\begin{aligned} C_1 &= -\frac{1}{z_{31}^2} \left[\frac{z_{31}(z_1^3 + z_1^2(z_4 - 2z_3)) + z_1 z_2(z_3 - 2z_4) + z_2 z_3 z_4}{z_{41} z_{21}} + \frac{z_1 z_{32} z_{43} f'(\eta)}{z_{42} f(\eta)} \right], \\ C_2 &= \frac{1}{z_{42}^2} \left[\frac{z_{42}(z_2^3 + z_2^2(z_3 - 2z_4)) + z_1 z_2(z_4 - 2z_3) + z_1 z_3 z_4}{z_{32} z_{21}} + \frac{z_2 z_{41} z_{43} f'(\eta)}{z_{31} f(\eta)} \right], \\ C_3 &= -\frac{1}{z_{31}^2} \left[\frac{z_{31}(z_3^3 + (z_2 - 2z_1)z_3^2 + (z_1 - 2z_2)z_4 z_3 + z_1 z_2 z_4)}{z_{43} z_{32}} + \frac{z_3 z_{21} z_{41} f'(\eta)}{z_{42} f(\eta)} \right], \\ C_4 &= \frac{1}{z_{42}^2} \left[\frac{z_{42}(z_4^3 + (z_1 - 2z_2)z_4^2 + (z_2 - 2z_1)z_3 z_4 + z_1 z_2 z_3)}{z_{41} z_{43}} + \frac{z_4 z_{21} z_{32} f'(\eta)}{z_{31} f(\eta)} \right]. \quad (\text{A12}) \end{aligned}$$

Once again the nonlogarithmic terms described by Eq. (A11) vanish on insertion of the limits of integration $\tau = 0$ and $\tau = \beta$, whereas the logarithmic terms in Eq. (A10) contribute according to the relation in Eq. (A4), which modifies the limits of the integration over x as follows:

$$\int_{-\infty}^{\infty} dx \rightarrow \int_{-\frac{\beta}{2\pi} \log z_j}^{\infty} dx, \quad j = 1, 2, 3, 4. \quad (\text{A13})$$

The integration over x for the integrand in Eq. (A10) may now be performed with the modified limits described above to arrive at

$$-\frac{\beta^2}{2\pi} \sum_{j=1}^4 C_j \log z_j. \quad (\text{A14})$$

The desired correction to the OEE of a single interval of length ℓ may now be obtained through the substitutions $\{z_1, z_2, z_3, z_4\} \rightarrow \{e^{-\frac{2\pi\ell}{\beta}}, e^{-\frac{2\pi\ell}{\beta}}, 1, e^{\frac{2\pi\ell}{\beta}}\}$ and subsequent implementation of the bipartite limit $L \rightarrow \infty$ as follows:

$$\begin{aligned} \lim_{L \rightarrow \infty} \int_{\mathcal{M}} d^2 w \sum_{j=1}^4 \left[\frac{z^2}{(z - z_j)^2} - \frac{z^2}{(z - z_j)} \partial_{z_j} \log [z_{23}^2 z_{41}^2 \eta f(\eta)] \right] \\ = \ell \beta \left(-\frac{1}{(e^{\frac{2\pi\ell}{\beta}} - 1)} + e^{-\frac{2\pi\ell}{\beta}} \frac{f'[e^{-\frac{2\pi\ell}{\beta}}]}{2f[e^{-\frac{2\pi\ell}{\beta}}]} \right) \\ - \lim_{L \rightarrow \infty} \left[L \beta \coth \left(\frac{2\pi L}{\beta} \right) \right]. \end{aligned} \quad (\text{A15})$$

As before the antiholomorphic part of the integral produces identical result to the holomorphic part.

-
- [1] S. Ryu and T. Takayanagi, Holographic derivation of entanglement entropy from AdS/CFT, *Phys. Rev. Lett.* **96**, 181602 (2006).
 - [2] S. Ryu and T. Takayanagi, Aspects of holographic entanglement entropy, *J. High Energy Phys.* **08** (2006) 045.
 - [3] V.E. Hubeny, M. Rangamani, and T. Takayanagi, A covariant holographic entanglement entropy proposal, *J. High Energy Phys.* **07** (2007) 062.
 - [4] D. V. Fursaev, Proof of the holographic formula for entanglement entropy, *J. High Energy Phys.* **09** (2006) 018.
 - [5] H. Casini, M. Huerta, and R. C. Myers, Towards a derivation of holographic entanglement entropy, *J. High Energy Phys.* **05** (2011) 036.
 - [6] A. Lewkowycz and J. Maldacena, Generalized gravitational entropy, *J. High Energy Phys.* **08** (2013) 090.
 - [7] X. Dong, A. Lewkowycz, and M. Rangamani, Deriving covariant holographic entanglement, *J. High Energy Phys.* **11** (2016) 028.
 - [8] K. Tamaoka, Entanglement wedge cross section from the dual density matrix, *Phys. Rev. Lett.* **122**, 141601 (2019).
 - [9] K. Babaei Velni, M.R. Mohammadi Mozaffar, and M.H. Vahidinia, Some aspects of entanglement wedge cross-section, *J. High Energy Phys.* **05** (2019) 200.
 - [10] Y. Kusuki and K. Tamaoka, Entanglement wedge cross section from CFT: Dynamics of local operator quench, *J. High Energy Phys.* **02** (2020) 017.
 - [11] J. Angel-Ramelli, C. Berthiere, V.G.M. Puletti, and L. Thorlacius, Logarithmic negativity in quantum Lifshitz theories, *J. High Energy Phys.* **09** (2020) 011.
 - [12] A. Mollabashi and K. Tamaoka, A field theory study of entanglement wedge cross section: Odd entropy, *J. High Energy Phys.* **08** (2020) 078.
 - [13] K. Babaei Velni, M.R. Mohammadi Mozaffar, and M.H. Vahidinia, Evolution of entanglement wedge cross section following a global quench, *J. High Energy Phys.* **08** (2020) 129.
 - [14] C. Berthiere, H. Chen, Y. Liu, and B. Chen, Topological reflected entropy in Chern-Simons theories, *Phys. Rev. B* **103**, 035149 (2021).
 - [15] X. Dong, X.-L. Qi, and M. Walter, Holographic entanglement negativity and replica symmetry breaking, *J. High Energy Phys.* **06** (2021) 024.
 - [16] M. Sahraei, M. J. Vasli, M. R. M. Mozaffar, and K. B. Velni, Entanglement wedge cross section in holographic excited states, *J. High Energy Phys.* **08** (2021) 038.
 - [17] M. Ghasemi, A. Naseh, and R. Pirmoradian, Odd entanglement entropy and logarithmic negativity for thermofield double states, *J. High Energy Phys.* **10** (2021) 128.
 - [18] J. K. Basak, H. Chourasiya, V. Raj, and G. Sengupta, Odd entanglement entropy in Galilean conformal field theories and flat holography, *Eur. Phys. J. C* **82**, 1050 (2022).
 - [19] A. B. Zamolodchikov, Expectation value of composite field T anti-T in two-dimensional quantum field theory, [arXiv: hep-th/0401146](https://arxiv.org/abs/hep-th/0401146).
 - [20] L. McGough, M. Mezei, and H. Verlinde, Moving the CFT into the bulk with $T\bar{T}$, *J. High Energy Phys.* **04** (2018) 010.
 - [21] V. Shyam, Background independent holographic dual to $T\bar{T}$ deformed CFT with large central charge in 2 dimensions, *J. High Energy Phys.* **10** (2017) 108.
 - [22] P. Kraus, J. Liu, and D. Marolf, Cutoff AdS₃ versus the $T\bar{T}$ deformation, *J. High Energy Phys.* **07** (2018) 027.
 - [23] W. Cottrell and A. Hashimoto, Comments on $T\bar{T}$ double trace deformations and boundary conditions, *Phys. Lett. B* **789**, 251 (2019).
 - [24] M. Taylor, TT deformations in general dimensions, [arXiv:1805.10287](https://arxiv.org/abs/1805.10287).
 - [25] T. Hartman, J. Kruthoff, E. Shaghoulian, and A. Tajdini, Holography at finite cutoff with a T^2 deformation, *J. High Energy Phys.* **03** (2019) 004.
 - [26] V. Shyam, Finite cutoff AdS₅ holography and the generalized gradient flow, *J. High Energy Phys.* **12** (2018) 086.

- [27] P. Caputa, S. Datta, and V. Shyam, Sphere partition functions & cut-off AdS, *J. High Energy Phys.* **05** (2019) 112.
- [28] A. Giveon, N. Itzhaki, and D. Kutasov, A solvable irrelevant deformation of AdS₃/CFT₂, *J. High Energy Phys.* **12** (2017) 155.
- [29] M. Asrat, A. Giveon, N. Itzhaki, and D. Kutasov, Holography beyond AdS, *Nucl. Phys.* **B932**, 241 (2018).
- [30] W. Donnelly and V. Shyam, Entanglement entropy and $T\bar{T}$ deformation, *Phys. Rev. Lett.* **121**, 131602 (2018).
- [31] A. Lewkowycz, J. Liu, E. Silverstein, and G. Torroba, $T\bar{T}$ and EE, with implications for (A)dS subregion encodings, *J. High Energy Phys.* **04** (2020) 152.
- [32] B. Chen, L. Chen, and P.-X. Hao, Entanglement entropy in $T\bar{T}$ -deformed CFT, *Phys. Rev. D* **98**, 086025 (2018).
- [33] A. Banerjee, A. Bhattacharyya, and S. Chakraborty, Entanglement entropy for TT deformed CFT in general dimensions, *Nucl. Phys.* **B948**, 114775 (2019).
- [34] H.-S. Jeong, K.-Y. Kim, and M. Nishida, Entanglement and Rényi entropy of multiple intervals in $T\bar{T}$ -deformed CFT and holography, *Phys. Rev. D* **100**, 106015 (2019).
- [35] C. Murdia, Y. Nomura, P. Rath, and N. Salzetta, Comments on holographic entanglement entropy in TT deformed conformal field theories, *Phys. Rev. D* **100**, 026011 (2019).
- [36] C. Park, Holographic entanglement entropy in cutoff AdS, *Int. J. Mod. Phys. A* **33**, 1850226 (2019).
- [37] M. Asrat, Entropic c -functions in $T\bar{T}$, $J\bar{T}$, $T\bar{J}$ deformations, *Nucl. Phys.* **B960**, 115186 (2020).
- [38] S. He and H. Shu, Correlation functions, entanglement and chaos in the $T\bar{T}/J\bar{T}$ -deformed CFTs, *J. High Energy Phys.* **02** (2020) 088.
- [39] S. Grieninger, Entanglement entropy and $T\bar{T}$ deformations beyond antipodal points from holography, *J. High Energy Phys.* **11** (2019) 171.
- [40] S. Khoeini-Moghaddam, F. Omid, and C. Paul, Aspects of hyperscaling violating geometries at finite cutoff, *J. High Energy Phys.* **02** (2021) 121.
- [41] M. Asrat and J. Kudler-Flam, $T\bar{T}$, the entanglement wedge cross section, and the breakdown of the split property, *Phys. Rev. D* **102**, 045009 (2020).
- [42] D. Basu, Lavish, and B. Paul, Entanglement negativity in $T\bar{T}$ -deformed CFT₂s, *Phys. Rev. D* **107**, 126026 (2023).
- [43] F. A. Smirnov and A. B. Zamolodchikov, On space of integrable quantum field theories, *Nucl. Phys.* **B915**, 363 (2017).
- [44] A. Cavaglià, S. Negro, I. M. Szécsényi, and R. Tateo, $T\bar{T}$ -deformed 2D quantum field theories, *J. High Energy Phys.* **10** (2016) 112.
- [45] J. Kudler-Flam, Y. Kusuki, and S. Ryu, Correlation measures and the entanglement wedge cross-section after quantum quenches in two-dimensional conformal field theories, *J. High Energy Phys.* **04** (2020) 074.
- [46] P. Calabrese, J. Cardy, and E. Tonni, Entanglement negativity in quantum field theory, *Phys. Rev. Lett.* **109**, 130502 (2012).
- [47] P. Calabrese, J. Cardy, and E. Tonni, Entanglement negativity in extended systems: A field theoretical approach, *J. Stat. Mech.* (2013) P02008.
- [48] P. Calabrese, J. Cardy, and E. Tonni, Finite temperature entanglement negativity in conformal field theory, *J. Phys. A* **48**, 015006 (2015).
- [49] J. Kumar Basak, H. Parihar, B. Paul, and G. Sengupta, Covariant holographic negativity from the entanglement wedge in AdS₃/CFT₂, *Phys. Lett. B* **834**, 137451 (2022).
- [50] B. Czech, J. L. Karczmarek, F. Nogueira, and M. Van Raamsdonk, The gravity dual of a density matrix, *Classical Quantum Gravity* **29**, 155009 (2012).
- [51] A. C. Wall, Maximin surfaces, and the strong subadditivity of the covariant holographic entanglement entropy, *Classical Quantum Gravity* **31**, 225007 (2014).
- [52] M. Headrick, V. E. Hubeny, A. Lawrence, and M. Rangamani, Causality & holographic entanglement entropy, *J. High Energy Phys.* **12** (2014) 162.
- [53] T. Takayanagi and K. Umemoto, Entanglement of purification through holographic duality, *Nat. Phys.* **14**, 573 (2018).
- [54] P. Calabrese and J. L. Cardy, Entanglement entropy and quantum field theory, *J. Stat. Mech.* (2004) P06002.
- [55] P. Calabrese and J. Cardy, Entanglement entropy and conformal field theory, *J. Phys. A* **42**, 504005 (2009).
- [56] A. L. Fitzpatrick, J. Kaplan, and M. T. Walters, Universality of long-distance AdS physics from the CFT bootstrap, *J. High Energy Phys.* **08** (2014) 145.
- [57] P. Francesco, P. Mathieu, and D. Sénéchal, *Conformal Field Theory* (Springer Science & Business Media, New York, 2012).
- [58] M. Banados, Three-dimensional quantum geometry and black holes, *AIP Conf. Proc.* **484**, 147 (1999).
- [59] S. Carlip, The (2 + 1)-dimensional black hole, *Classical Quantum Gravity* **12**, 2853 (1995).
- [60] S. H. Shenker and D. Stanford, Black holes and the butterfly effect, *J. High Energy Phys.* **03** (2014) 067.
- [61] J. D. Brown and M. Henneaux, Central charges in the canonical realization of asymptotic symmetries: An example from three-dimensional gravity, *Commun. Math. Phys.* **104** (1986) 207.
- [62] J. Kumar Basak, V. Malvimat, H. Parihar, B. Paul, and G. Sengupta, On minimal entanglement wedge cross section for holographic entanglement negativity, [arXiv:2002.10272](https://arxiv.org/abs/2002.10272).
- [63] D. Basu, A. Chandra, V. Raj, and G. Sengupta, Entanglement wedge in flat holography and entanglement negativity, *SciPost Phys. Core* **5**, 013 (2022).
- [64] D. Basu, H. Parihar, V. Raj, and G. Sengupta, Entanglement negativity, reflected entropy, and anomalous gravitation, *Phys. Rev. D* **105**, 086013 (2022).
- [65] X. Jiang, P. Wang, H. Wu, and H. Yang, Timelike entanglement entropy and TT^- deformation, *Phys. Rev. D* **108**, 046004 (2023).